Construction and Building Materials 407 (2023) 133479

Contents lists available at ScienceDirect

Construction and Building Materials

journal homepage: www.elsevier.com/locate/conbuildmat

Utilization of recycled concrete aggregates for developing high-performance and durable flexible pavements

Merve Akbas *, Bilal Ozaslan, Recep Iyisan

Istanbul Technical University, Civil Engineering Faculty, 34469 Maslak, Istanbul, Turkey

ARTICLE INFO

Keywords:
RCA
Durable pavement
Resilient modulus
3D nonlinear analysis
Rutting
Freeze and thaw

ABSTRACT

The objective of this research was to explore the feasibility of using recycled concrete aggregates (RCA) to construct flexible pavements with high performance and durability. The research is based on materials obtained from urban renewal projects in Istanbul, where RCA can be sourced from construction demolition waste. The grain diameter distributions of subbase and base samples, intended for road infrastructure implementation, were established to comply with the AASHTO Pavement Structures Design Guidelines specifications. Laboratory tests were conducted to determine the physical, mechanical, and stiffness properties of subbase and base samples prepared with RCA. In addition, the influence of freeze–thaw (F-T) cycles on the stiffness characteristics of RCA was examined experimentally through resilient modulus and permanent deformation tests carried out on base and subbase samples subjected to a range of 1 to 20F-T cycles. Also, numerical evaluations were undertaken using finite difference numerical modeling software to investigate the mechanical performance of flexible pavements built with RCA under significant loads, utilizing parameters derived after various numbers of F-T cycles. The findings suggest that the stiffness properties of RCA meet the required specifications for subbase and base materials after F-T cycles, indicating that RCA can potentially provide high performance in flexible pavement construction under varying environmental conditions.

1. Introduction

The demand for new infrastructure due to growing populations and the significant amount of solid waste generated, primarily by the construction industry, place significant pressure on the environment. Due to the scarcity of high-quality materials and the rising cost of natural aggregate, construction and demolition waste (C&D) is increasingly being recognized as a valuable resource [1–5]. Recycled Concrete Aggregates (RCA), which account for approximately 70% of construction waste, have been shown to be especially useful for developing high-performance and durable flexible pavements [6].

The Pavement Mechanistic-Empirical Design (PMED) approach is used in designing flexible pavements that considers course stiffness, climate zone, traffic conditions, the intended service life of the pavement, and damage criteria to create a sustainable pavement design. Material input parameters are used in the PMED approach for empirical prediction models, and pavement deteriorations such as rutting, fatigue cracking, thermal cracking, and roughness are analyzed to evaluate the deformations that will occur at mechanically determined critical stresses depending on temperature and humidity levels. Accurate traffic, climate, and material input parameters ensure that the coating stresses and deformations that will occur at critical locations in the system are as close to reality as possible. The resilient modulus and permanent deformation are stiffness properties used as material inputs for the pavement response model to measure the stress-induced resilience of unbonded materials under moving wheel loads [7].

While many studies have examined the mechanical and strength properties of RCA, few studies have focused on the stiffness properties of RCA and its freeze and thaw (F-T) effects on the mechanical behavior of pavement courses under moving wheel loads [8,9]. Studies on recycled aggregates and natural soils have shown that F-T has an impact on both the resilient modulus and the permanent deformation of the aggregates. For instance, Li et al. [10] examined the factors influencing the elasto-plastic behavior of RCA subjected to F-T. Their results indicate that the initial stress ratio, initial average stress, repeated stress amplitude, temperature, and initial water content affect permanent deformation values. Rosa et al. [11] showed that the resilient modulus of RCA increases up to a certain cycle and then decreases. Bassani and Tefa [12]

* Corresponding author at: Istanbul Technical University ITU, Civil Engineering Faculty, Geotechnical Engineering, Ayazaga Campus, 34469 Maslak, Istanbul, Turkey.

E-mail addresses: akbasm@itu.edu.tr (M. Akbas), ozaslanb@itu.edu.tr (B. Ozaslan), iyisan@itu.edu.tr (R. Iyisan).

https://doi.org/10.1016/j.conbuildmat.2023.133479
Received 19 June 2023; Received in revised form 16 September 2023; Accepted 20 September 2023
Available online 27 September 2023

demonstrated that the resilient modulus of concrete and brick aggregates obtained from construction waste decreases with increasing F-T cycles.

The understanding of F-T damage mechanisms and the evaluation of the performance of pavement structures under different environmental conditions, including F-T cycles, are essential for the design and maintenance of resilient and durable pavements [13–16]. In recent years, research has focused on the effects of F-T cycles on the strength, durability, and mechanical properties of pavement materials, all of which can have significant implications for pavement performance and should be considered in pavement design and maintenance practices [17–19]. However, although the use of numerical simulations to analyze the mechanical behavior of pavement structures has been explored in recent years [20–22]; studies that use parameters obtained from experiments in 3D numerical simulations of pavement structure, enabling examination of the pavement's mechanical behavior under a moving wheel load and different F-T conditions, not included in the literature. Furthermore, elastic theory with the Mohr-Coulomb failure criterion has been used by researchers to model the permanent deformation behavior of pavement granular soils under cyclic loading [23,24]. Mohammadinia et al. [25] stated that elastic theory cannot be used to model the stress dependence of soil stiffness. Pérez et al. [26], for example, observed the peak responses at critical positions of pavement course sections using the FLAC3D code in an axisymmetric approach. They concluded that base courses with natural and recycled aggregates exhibit similar nonlinear behavior due to the nonlinear behavior of the base courses with natural and recycled aggregates and their dependence on stresses on their resilient modulus. However, Akbas et al. [27] suggested that 3D models can provide more accurate outcomes than axisymmetric methods. They attributed this to the restrictions caused by the short length of the slope on the side and the complex interactions among the various dynamic effects of a moving vehicle's different axes.

The aim of this study was to investigate the potential for utilizing recycled concrete aggregates (RCA) in the development of high-performance and durable flexible pavements. Specifically, the stiffness properties of RCA and their behavior under F-T cycles were examined, as they were key factors in determining the long-term performance of pavement structures. Laboratory tests were conducted on subbase and base samples prepared with RCA to determine their hydraulic, mechanical, and stiffness properties, including resilient modulus and permanent deformation. Additionally, the F-T effect on the stiffness properties of RCA was evaluated by subjecting samples to varying numbers of F-T cycles. Numerical modeling was used to assess the mechanical behavior of flexible pavements constructed with RCA under substantial loads. The parameters obtained from laboratory tests and F-T experiments were utilized to create 3D models in FLAC3D, a finite difference numerical modeling software. Overall, this study aimed to contribute to the growing body of research on the use of RCA in pavement construction and to provide insights into the potential of these materials for developing sustainable and high-performance infrastructure. By investigating the stiffness properties of RCA and their behavior under F-T cycles, valuable information on the performance and durability of flexible pavements constructed with recycled materials was provided to pavement designers and engineers.

2. Material and methods

2.1. Physical and geotechnical properties of RCA

Construction and demolition wastes (C&D) were collected from different building sites in Istanbul with a maximum nominal grain size of 3 cm. The collected waste containing various impurities was crushed in a plant and separated based on type, such as brick, concrete, metals, etc. Recycled concrete aggregates (RCA) were obtained from the concrete debris, and their physical properties were determined to illustrate their characteristics.

The soundness of the aggregates was particularly evaluated using the ASTM C88 test method with sodium sulfate (Na2SO4) to understand the performance of RCA under different environmental conditions. This standard procedure involves subjecting aggregates to repeated immersion in a saturated solution of sodium sulfate, followed by oven-drying. The five cycle was repeated multiple times to simulate the effects of environmental conditions on the aggregates. At the conclusion of the test cycles, the aggregates were sieved and the percentage of weight loss is determined. Moreover, the Los Angeles abrasion coefficient (LA), flakiness index (FI), water absorption (WA24), clay lumps and friable particles in aggregates (%), and methylene blue index of clay were also evaluated to determine the physical properties of the RCA materials. In experiments requiring fine materials, materials that passed the #200 sieve (or 75 μm) were used, constituting approximately 5–6% of the sample. The physical properties of the RCA materials obtained were compared to the relevant specifications. Table 1 summarizes the physical properties of the RCA materials based on the specifications with the grain size distribution parameters.

The particle size distribution for the received RCA sample was evaluated using a sieve analysis in accordance with the standards set by ASTM D3282. The classification for the material was determined to be SP-SM (Poorly-Graded Sands with Silt) and A-1-b (Granular Soils), as per the criteria of the Unified Soil Classification System (USCS) outlined in ASTM D2487 and the AASHTO Soil Classification System outlined in AASHTO M145, respectively. The particle size distribution for the received RCA sample was evaluated using a sieve analysis in accordance with the standards set by ASTM D3282. The classification for the material was determined to be SP-SM and A-1-b, as per the criteria of the Unified Soil Classification System (USCS) and AASHTO Soil Classification System, respectively, outlined in ASTM D2487 and AASHTO M145. The grain size distribution of the initial samples was found to be incompatible with the AASHTO Guide for Design of Pavement Structures (1993) limits [28], necessitating the derivation of new grain size distributions for the base and subbase course samples. Consequently, the original material underwent laboratory sieving to yield aggregates of diverse grain diameters. The aggregates thus obtained were then mixed in different proportions to prepare subbase and base samples that conformed to the relevant grain size distribution specifications.

All samples underwent evaluations to determine their geotechnical properties such as specific gravity, optimum moisture content (w_{opt}), maximum dry unit weight (γ_{dmax}), hydraulic conductivity (k), friction angle (ϕ), and cohesion intercept (c). The results of the specific gravity, standard and modified Proctor, constant head, and direct shear tests, which were conducted in line with ASTM D854, ASTM D698 and ASTM D1557, ASTM D2434, and ASTM D3080 respectively, are presented in Table 2 alongside the classification features of the base and subbase samples. The Atterberg limit test results affirmed that all samples were identified as non-plastic materials.

Table 1
Physical properties of the recycled aggregates.

Physical Property	Specification	Result	Relevant Specification
Soundness	≤10% for Na2SO4, ≤15% for MgSO4	5.5%	ASTM C88
LA Abrasion Coefficient	≤50%	22.4%	ASTM C131
Flakiness Index	≤35%	12.8%	BS EN 933-3
Water Absorption (WA24)	≤2.0%	1.6%	ASTM C127
Clay Lumps and Friable Particles	≤3.0%	0.8%	ASTM C142
Methylene Blue Index of Clay	≤4.0 mg/g	2.2 mg/g	ASTM C837

Table 2
Geotechnical properties of the samples.

Properties	Subbase	Base
AASHTO	A-1-a	A-1-a
USCS	GW-GM	GW-GM
Gravel (%) (D>4.76 mm)	50	62
Sand (%) (0.074 mm<D<4.76 mm)	44	33
Fines Content (%) (0.074 mm)	6	5
C_u	50.66	65.5
C_c	1.48	2.80
$\gamma_{d\ max-standart}$ (kN/m^3)	19.40	20.10
$w_{opt-standart}$ (%)	11	10
$\gamma_{d\ max-modified}$ (kN/m^3)	19.80	20.50
$w_{opt-modified}$ (%)	8	7
k (m/s)	5.64 x 10^{-5}	5.87 x 10^{-5}
ϕ(°)	32	48
c (kPa)	28	10
Soaked CBR (%)	121	133
Unsoaked CBR (%)	106	109

2.2. Experimental methods

The laboratory tests conducted in this study aimed to determine the hydraulic, mechanical, and stiffness properties of the subbase and base samples prepared with RCA. The resilient modulus, and permanent deformation tests were conducted to evaluate the stiffness and plastic deformation (rutting) performance of the samples under varying environmental conditions. The freeze and thaw (F- T) experiments were carried out to assess the effect of F-T cycles on the stiffness properties of RCA and their potential limitations in road construction.

2.2.1. Resilient modulus tests and used models to estimate the resilient modulus

The resilient modulus test was carried out according to the AASHTO T307 method [29], which measures the resilience of the material under repetitive loads. The test involved compressing a sample into a cylindrical mold under conditions that replicate those expected in the field. Unprocessed granular base and subbase materials are classified as Type-1 and Type-2 based on sieve analysis and Atterberg limit test results. Samples of subbase and base materials, where the percentages of particles passing through the No 10 (2 mm) sieve and the No 200 (0.074 mm) sieve are less than 70% and 20%, respectively, and have a plasticity index of less than 10%, are defined as Type-1. After compaction, the sample was placed in a triaxial chamber where it was subjected to confining pressure, simulating the lateral pressures of a real-world pavement structure. The core of the test involved applying a cyclic axial load on the specimen, replicating the burdens exerted by moving traffic. The resilient modulus was derived by analyzing the recoverable axial strain resulting from the applied axial stress. Conducted under diverse combinations of stresses, the results provide a comprehensive mathematical model or relationship that describes the behavior of the material. Furthermore, this study used several models to estimate the resilient modulus of the RCA materials. These models include the Power model proposed by Hicks and Monismith [30], the Uzan model proposed by Uzan [31], and the Mechanical-Empirical Pavement Design in NCHRP 1-37A [32].

The Power model calculates the resilient modulus as a function of the stress applied and the stiffness of the material. The Uzan model is based on the Power model but also considers the effect of atmospheric pressure on the resilient modulus. The Mechanical-Empirical Pavement Design (MEPD) model considers both atmospheric pressure and the octahedral shear stress on the resilient modulus.

The equations for the three models are given in Equations 2.1, 2.2, and 2.3, respectively. The constants k_1, k_2, and k_3 in each equation are determined using best-fit analysis. The deviator stress (σ_d) and atmospheric pressure (P_a) are also included in the equations.

$$\text{Power}: M_R = k_1\theta^{k_2} \quad (2.1)$$

$$\text{Uzan}: M_R = k_1 P_a(\theta/P_a)^{k_2}(\sigma_d/P_a)^{k_3} \quad (2.2)$$

$$\text{MEPD}: M_R = k_1 P_a(\theta/P_a)^{k_2}(\tau_{oct}/P_a + 1)^{k_3} \quad (2.3)$$

Equations 2.4, 2.5 and 2.6 describe how the total stress (θ), octahedral shear stress (τ_{oct}) and σ_d are related to the principal stresses (σ_1, σ_2, and σ_3). These equations were used to calculate the stresses necessary for the resilient modulus calculations.

$$\theta = \sigma_1 + \sigma_2 + \sigma_3 \quad (2.4)$$

$$\tau_{oct} = \frac{1}{3}\sqrt{(\sigma_1-\sigma_2)^2 + (\sigma_1-\sigma_3)^2 + (\sigma_2-\sigma_3)^2} \quad (2.5)$$

$$\sigma_d = \sigma_1 - \sigma_3 \quad (2.6)$$

2.2.2. Permanent deformation tests

In addition to the resilient modulus test, permanent deformation tests were also conducted on the prepared subbase and base samples. The samples were subjected to repetitive loads at a constant strain level for a specific number of cycles, and the permanent deformation was measured. According to NCHRP report 01-28A, the permanent deformation test started with the same initial loading as the resilient modulus test and continued with 10,000 repetitions of a load with a confining pressure (σ_3) of 34.5 kPa and a σ_d of 206.8 kPa.

2.2.3. F-T tests

The F-T tests were carried out to assess the effect of F-T cycles on the stiffness properties of RCA and their potential limitations in road construction. F-T tests were conducted on the subbase and base samples according to ASTM D6035. The samples were wrapped in stretch film to prevent water loss during the F-T cycling, which involved 24 h of freezing at −20 °C and 24 h of thawing at 20 °C. The stiffness characteristics of the RCA samples were assessed after 1, 3, 5, 10, and 20F-T cycles, consistent with other research in the literature [11,27]. Moreover, the model exhibiting the best concurrence between lab-measured and predicted modulus was selected for numerical analysis.

2.3. Numerical methods

The Mechanistic Design of pavement structures is a state-of-the-art process for the design of pavement structures. The methodology of the mechanistic pavement design approach has been established by the NCHRP one (NCHRP 2004) design procedure [32], which is different from the AASHTO 1993 design method [28] with respect to the inclusion of numerical analysis based on the theories of mechanics. The mechanistic design of new pavement structures according to NCHRP 1-37A [32] consists of several steps, which are: defining the traffic load, selecting a pavement section, assigning the properties for the materials in the pavement courses, analyzing the pavement response (stress, strain) due to traffic loading for different seasons (temperature, moisture), relating to the empirically determined pavement response, comparing the predicted distresses against design limits, adjusting the pavement section if necessary [33,34].

Pavement analyses were conducted using a fully nonlinear approach that relies on an explicit finite difference scheme, and it resolves complete equations of motion through the FLAC3D code. We selected the finite difference method for the analyses due to its flexibility in representing irregular geometries. Furthermore, the fully nonlinear method accommodates any specified nonlinear constitutive relationship. In this method, plastic yielding was appropriately modeled, as strain increments (not tensors) are linked to stress tensors. We intentionally designed the model length to be considerably longer than that of a standard truck. The constructed three-dimensional mesh model comprised more than 235,000 hexahedral zones. For the pavement models, we implemented advanced boundary conditions to mitigate irregular overburden and stress concentrations near the boundaries. A

schematic illustration of the pavement model is presented in Fig. 1. At the bottom boundary, we applied the quiet-boundary scheme. For the lateral boundaries, we employed non-reflecting free-field boundaries connected through viscous dashpots to link the main grid with the free-field grid, as illustrated in Fig. 2.

2.3.1. Three-dimensional models of the flexible pavement and boundary conditions

In this section, the mechanical behavior of three-dimensional (3D) models of flexible pavement in which base and subbase courses were constructed by RCA has been investigated by the finite difference method (FDM). An elastoplastic model was applied to the subbase and base material using experimentally determined modules to capture the time-dependent non-linear behavior of the pavement under a dynamic load generated by the tire of a heavy truck. The elastic and plastic deformations of the sub courses, which underlie the elastic hot bituminous mixture course, were investigated according to the model standard. The load conditions for the analyses were established based on the multiple tire loading from a heavy truck. This truck configuration includes a single axle with a front wheelset and a double axle tandem with twin wheels, in line with the Federal Highway Administration (FHWA) vehicle classification schema. [35,36].

The cornerstone of numerical analysis lies in scrutinizing the responses of individual pavement courses to delineate the overall behavior of the pavement structure. In the computational procedures of NCHRP 1-37A [32] for flexible pavement analysis, structural responses are examined by considering critical stresses and deflections. During these analyses, the pavement models comprise different layers, each defined by distinct material properties but operating as a single, unified structure under load. One significant advantage of the 3D finite difference (FD) scheme utilized is that it allows for the exact positioning of multiple wheel loadings in 3D models. Consequently, the stress–strain behavior can be established, considering the automatic superposition of loadings under multiple wheels.

The model was constructed as a 10 m segment of a two-lane highway, with a pavement width (L) of 7 m on the surface and a total pavement depth (H) of 1 m above the subgrade. The HMA surface layer is 0.05 m thick, the base layer is 0.30 m, and the subbase layer is 0.65 m. The slope on the pavement edges was set at $\alpha = 45^{\circ}$, as depicted in Fig. 1. The subgrade depth was determined to be twice the thickness of the pavement to effectively monitor the stress distribution in the soil.

The accuracy of the results and the efficiency of time in the mesh construction is influenced just as much by proper element aspect ratios as it is by material non-linearity. In the analyses, the finite media is automatically discretized into hexahedral zones (meshes) by the code, and each zone is further divided into sets of tetrahedra. The mixed discretization technique is applied to counteract the excessively stiff behavior of uniform strain tetrahedral zones, which reach plastic flow [37].

The approach used in this investigation's loading conditions differs from those used in other studies under static loads. The loads were defined as dynamic wheel pressures under the truck axles' positions, manifested as a sinusoidal pulse in the time-domain. Therefore, due to the nature of the dynamic load excitation, advanced boundary conditions were assigned to all edges of the finite media, as shown in Fig. 2. Free-field boundaries were defined to prevent stress reflection on the lateral boundaries, and quiet-boundary conditions were used to connect the main grid to the infinite bottom using viscous dashpots. The dashpots produced viscous traction of shear and normal stresses, as explained by Equations 2.7, 2.8, 2.9, and 2.10.

$$F_x = -\rho\, C_p\, (v_x^m - v_x^{ff})\, A + F_x^{ff} \quad (2.7)$$

$$F_y = -\rho\, C_s\, (v_y^m - v_y^{ff})\, A + F_y^{ff} \quad (2.8)$$

$$t_n = -\rho\, C_p\, v_n \quad (2.9)$$

$$t_s = -\rho\, C_s\, v_s \quad (2.10)$$

Where F_x, F_y: the tractions of the free-field boundary. v_x^m, v_y^m: the velocities (x, y directions) of the gridpoint at the subgrade boundaries. v_x^{ff}, v_y^{ff}: the velocities (x, y directions) of the gridpoint in the additional free field sides. A: the influence area of the free-field gridpoint. F_x^{ff}, F_y^{ff}: free-field gridpoint forces (derived by xx, xy stresses from the free-field zones around the gridpoints. t_n, t_s: the normal and shear stresses traction, respectively, ρ is the mass density. C_p, C_s: the pressure and shear wave velocities. v_n, v_s: the normal and shear components of velocity at the quiet boundary [37,38].

2.3.2. Loading condition

Design approaches based on cumulative equivalent single-axle loads make it challenging to determine the horizontal locations of critical responses. Such a simple case of a single wheel load can only investigate the critical location of pavement response directly beneath the wheel's center. In actual pavement conditions, load configuration (which depends on multiple wheels/axles, vehicle types in mixed traffic conditions, and structural geometry including the number of lanes, edge slope, pavement width, and course thicknesses) will determine the critical location of pavement response. The NCHRP design methods propose a set of potential critical locations for examining pavement response, thereby addressing this issue. However, the effects of stress superposition from each wheel on the lanes cannot be observed. Furthermore, the strain interaction of pavement courses under total stresses, which comprise vehicle loads and pavement overburden

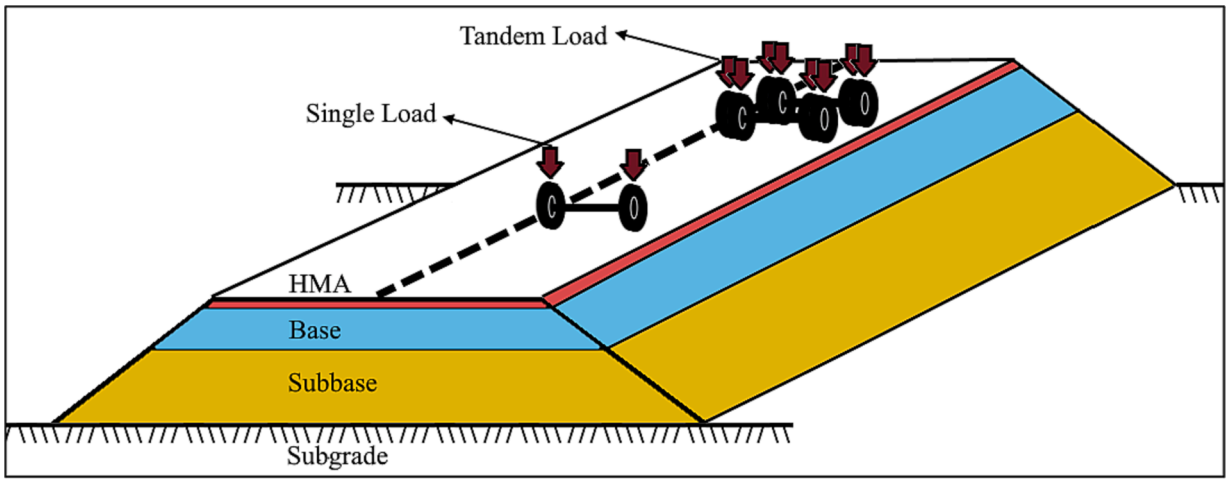

Fig. 1. The structure of coursed pavement and the positions of multiple axles loading conditions with single and double wheels.

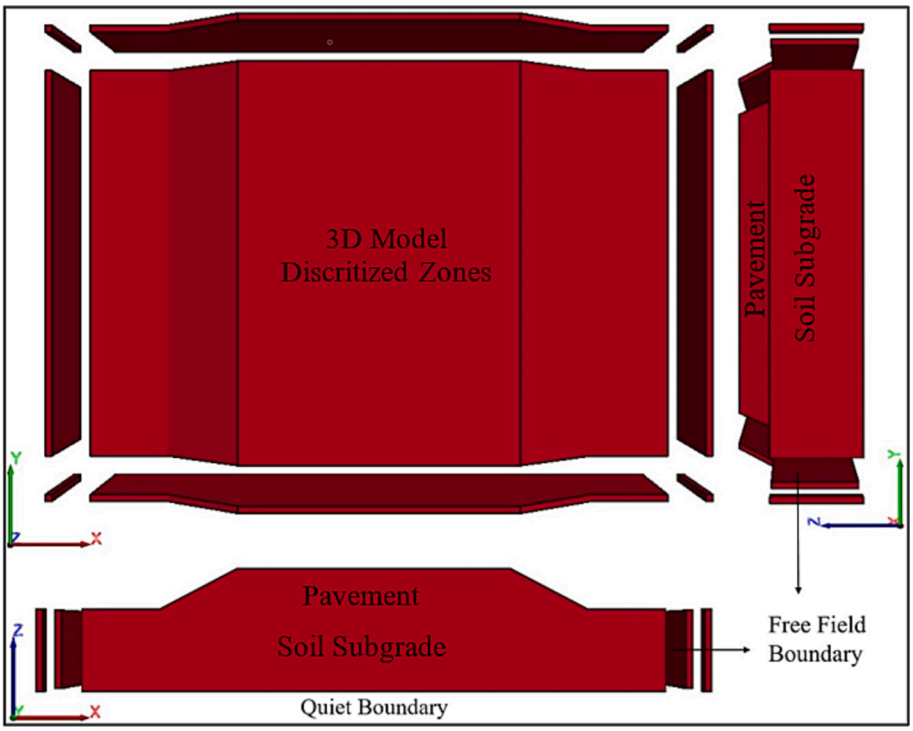

Fig. 2. The boundary conditions of 3D pavement model in Finite Difference Scheme.

stresses through course weights, cannot be inspected at the edge of the pavement slope. To account for these effects, analyses were performed in a three-dimensional space, assigning materials with nonlinear constitutive models under dynamically influenced multiple wheel loads [39].

In the analyses, the single axle load from two wheels, each with one tire, is transmitted via parallel stress planes 2 m apart, each having a contact surface of 0.4 m^2. The load transition from the tandem axle is defined similarly, but with two consecutive axles, each having four wheels with eight tires. The loads are defined as 1 MPa pressure stresses for all tire locations and are characterized by a sinusoidal pulse in the time-domain, as shown in Fig. 3 [27,40].

2.3.3. *Finite element analysis (FEM)*

Finite Element Analysis (FEM) is an advanced method that employs complex differential equations to calculate stress–strain relations throughout the defined media, approximating the solution of an engineering problem algebraically. Although the method has been proven to be a reliable procedure, computations may take days due to the implicit solutions of stored matrices. In contrast to the common implicit methods, the performed explicit solution with the finite difference scheme in the research can solve nonlinear problems in almost the same computer time as linear laws, even if the model has numerous elements. The mechanics of discrete elements in finite dimensions are derived from constitutive equations and laws of motion by given specific boundary and initial conditions. This method enables the examination of the combined effects of soil stress interference in pavement layers exposed to closely spaced, multiple loads. These effects, often omitted in simpler numerical studies like axisymmetric and plain-strain analyses, include variations in stress distribution and load-carrying capacity of the pavement structure. Numerical analyses can provide site-consistent results by defining nonlinear soil properties and advanced boundary conditions. Thus, it ensures the consideration of the effects of road section geometry, and multiple loading forms in dynamic conditions, on pavement performance during the design process [41].

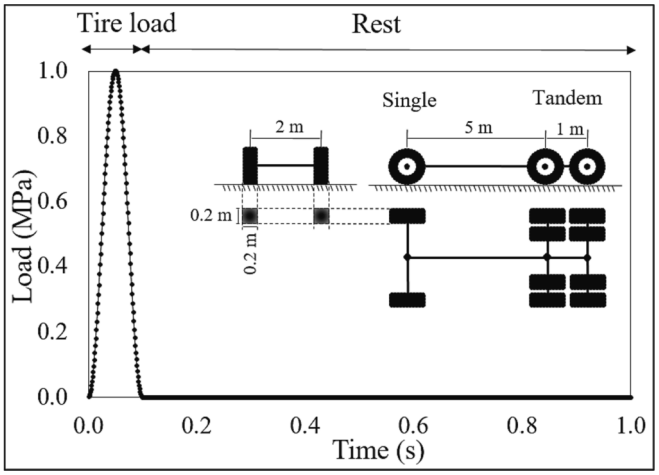

Fig. 3. Multiple loads with three axles in the time domain.

3. Results and discussion

3.1. *Effects of freeze–thaw cycles on resilient modulus and permanent deformation*

A laboratory study was conducted to investigate the effects of freeze–thaw (F-T) cycles on the resilient modulus and permanent deformation of pavement materials. These factors are known to influence pavement performance and durability. Control samples, consisting of subbase and base samples that were not exposed to any F-T cycles, were tested to provide a baseline for comparison. The resilient modulus and permanent deformation values of the base and subbase samples were then observed after 1, 3, 5, 10 and 20F-T cycles were administered.

In the resilient modulus tests, 15 load sequences were administered to the samples. In each sequence, the average modulus of resilience (MR) was determined from the last five cycles. These values were then aggregated and divided by 15 to ascertain the average MR for the sample. The resilient modulus and permanent deformation tests were

conducted after a specified number of F-T cycles. Fig. 4 displays the average values for both tests over the range of F-T cycles.

As expected, an increase in the resilient modulus with increasing bulk stress and an almost linear relationship between the bulk stresses and the resilient modulus were observed. In Fig. 4 (a), it is evident that the control base samples exhibit a higher average resilient modulus compared to the control subbase samples. As expected, an increase in the resilient modulus with increasing bulk stress and an almost linear relationship between the bulk stresses and the resilient modulus were observed. Specifically, the base samples displayed an average resilient modulus of 244.77 MPa, whereas the subbase samples showed an average of 219.99 MPa. This minor difference can be attributed to the particle size distribution and the fine content, which is slightly higher in the subbase samples. When the previous studies were examined, it was determined that these results were consistent. To illustrate, Mishra and Tutumluer [42] concentrated solely on the effect of gradation and noticed a slight decrease in the resilient modulus with fine content, proposing an optimum fine content around 5% for optimal stiffness. Moreover, Xiao et al. [43] revealed a gradual decrease in the resilient modulus of the recycled aggregates with an increasing relative content of fine particles at the same stress level. Previous studies have shown that the MR values of RCAs vary widely, being either higher or lower than the MR values obtained in this study [44,45]. For instance, Kallop et al., [46] reported MR values of the RCA samples studied as 114.95 MPa, while Yaghoubi et al. [47] stated the MR values of RCA as132 MPa in their analysis of the stress–strain response of pavement structures. Furthermore, Cancino [48] analyzed three RCAs, one from a plant-based source and two from recycled in-place construction sites in Oklahoma and observed an average resilient modulus ranging from approximately 81 MPa to 104.158 MPa. However, in the study carried out by Toka and Olgun [49], where they utilized different RCAs according to their parent concrete's compressive strength, the MR values were significantly higher than these previously mentioned MR values. The highest MR values they obtained averaged 200 MPa. In addition, Bozyurt et al. [50], examined the results of 64 laboratory and 5040 field tests for the MR values of RCA and stated that the average MR value for RCA was 320 ±

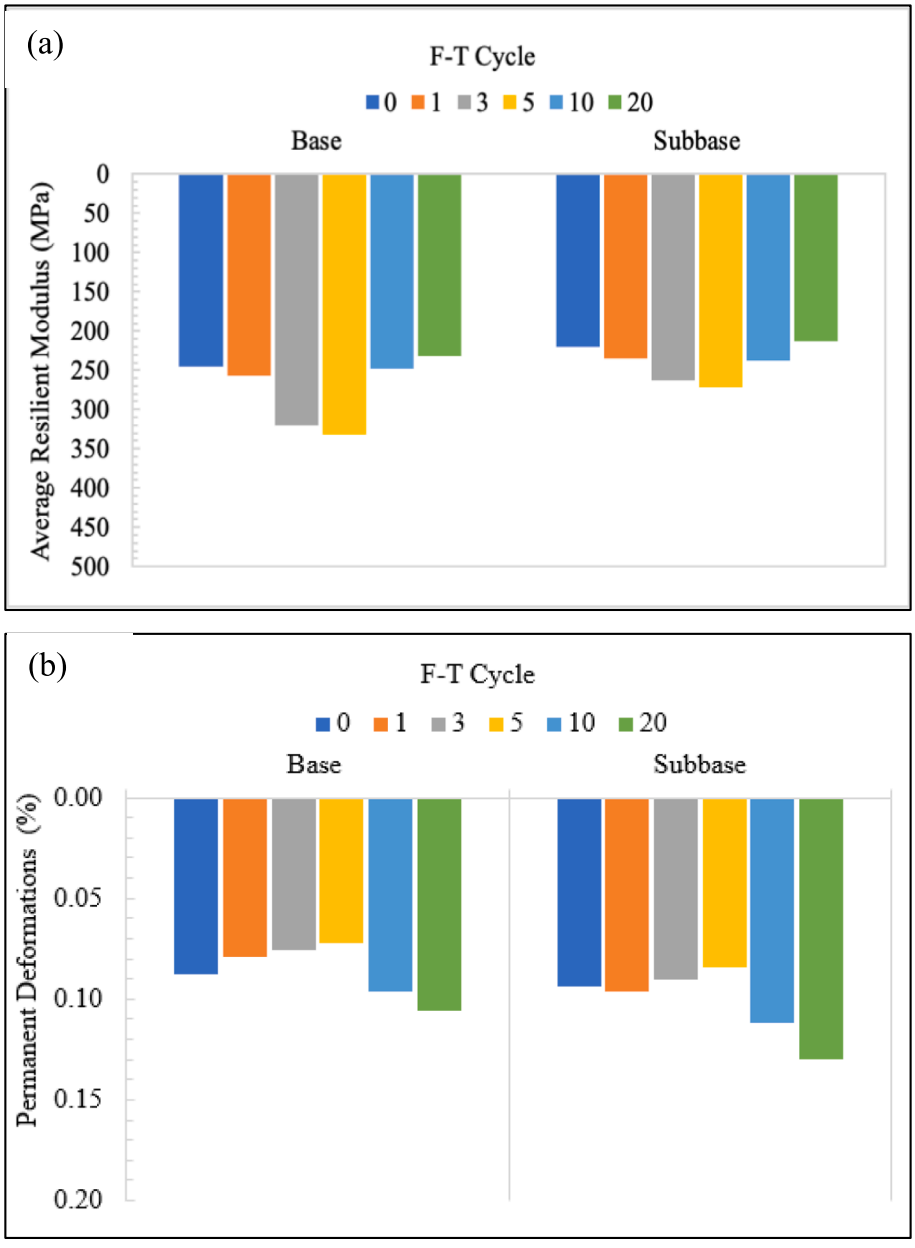

Fig. 4. The relationship between the average resilient modulus and the numbers of F-T cycles.

73 MPa. These results indicate that the MR values of the control sample are reasonable and specific to the recycled concrete aggregates used, and the quantitative values of the various parameters may differ when aggregates from different sources are used.

After the 1F-T, the base samples showed an increase from 244.77 MPa to 257.40 MPa, and the subbase samples experienced a similar increase from 219.99 MPa to 235.48 MPa. This upward trend continued through the 3 and 5F-T. The MR values peaked at the 5F-T, with the base samples registering 331.92 MPa, a 35% increase, and the subbase samples achieving 272.34 MPa, approximately a 24% increase, both based on the MR values of the control samples. However, after the 5F-T cycle, a downward trend was observed. By the 10F-T, the MR values had dropped to 237.11 MPa for the base samples and to 247.64 MPa for the subbase samples. This decline continued through the 20F-T, where the MR values further decreased to 232.54 MPa for the base samples and 212.61 MPa for the subbase samples, representing approximately 5% and 3% decreases, respectively, based on the MR values in the control samples. The increase in MR values up to a certain number of F-T cycles can be attributed to the fine particles in the RCA and additional fine particles generated by the F-T process, which act as a cementing agent in the presence of water during the sample preparation process. This occurs where the cement within the samples reacts with water to create a stronger, more resilient material up to a certain number of F-T cycles, due to the consolidating effect of partial densification from ice grain cohesion [51,52]. However, repeated exposure to F-T cycles leads to a weakening of the internal structure of the samples, or the soil skeleton. This is because the soil samples do not have enough pore space to endure freezing expansion without causing a change in microstructure [53,54].

In studies examining the effect of F-T cycles on the resilient modulus (MR) of recycled concrete aggregate (RCA) materials, various trends have been observed. Some studies indicate that the MR-F-T trend changes after a certain number of cycles, as observed in the study. On the other hand, the others indicate that the MR value may either decrease or increase with an increasing number of F-T cycles. For example, Soleimanbeigi et al. [55] conducted a study on RCAs obtained from different sources. MR values of RCAs showed decreasing trend from the initially up to 5F-T cycles and then increasing trend up to 20F-T, and this value higher about 28–36% more than its original values of before F-T. Rosa et al. [56] also observed a similar trend, with the MR of RCA materials decreasing after 5F-T cycles, followed by a consistent increase resulting in an approximately 35% increase in MR after 20F-T cycles. Zhang et al. [57] showed that the MR gradually decreased -range varied between 15% and 42%- due to repeated freezing and thawing and stabilized after 6F-T cycles, with the most significant damage occurring after the first F-T cycle. However, some studies have reported different trends and suggested that the MR value may either decrease or increase with an increasing number of F-T cycles. For instance, Daigna et al. [58] observed that the resilient modulus decreased 53% considering its original values of before F-T after 20F-T cycles of 100% RCA sourced from a concrete company in Green Bay, Wisconsin. Conversely, Ghorbani et al. [59] demonstrated that the application of F-T cycles consistently improved the MR of RCA and maintained its deformation properties after 20F-T cycles.

Moreover, even at the twentieth F-T cycle, the MR of recycled aggregates has been shown to be higher or comparable to that of virgin aggregate, as found in the literature. For instance, Titi and Mater [60] presented the resilient modulus of base course aggregates from Wisconsin and Kentucky, which involved both gravel/crushed gravel and crushed stone. The mean resilient modulus for aggregates from Wisconsin quarries was 164.02 MPa, while that from Wisconsin pits was 163.47 MPa. The mean resilient modulus for Kentucky aggregates was 282.27 MPa. Furthermore, Cancino [48] reported that the resilient modulus of the virgin limestone aggregate, which was collected from an aggregate quarry in Davis, Oklahoma, was approximately 105 MPa. Numerous investigations that have assessed the application of RCAs as a base and subbase for pavements have shown that the stiffness of the RCA either matches or surpasses that of virgin aggregates, a finding consistent with this study [61–64].

The permanent deformation values of the base and subbase samples after 10,000 load cycles under various F-T conditions are presented in Fig. 4 (b). Both the base and subbase samples showed a decreasing trend in permanent deformation values with increasing F-T cycles up to 5. For example, the base sample's deformation values reduced from 0.0875 at 0F-T cycles to 0.0720 at 5 F-T cycles – a 22% decrease. Meanwhile, the subbase sample decreased from 0.0940 to 0.0845, marking an 11% reduction. The gradual reduction in permanent deformation values for both the base and subbase samples can be attributed to the strengthening effect of cement hydration and increased interlocking between particles, leading to a more rigid structure and reduced deformation. The relatively stiffer region formed as a result of the reaction between excess cement and water surrounding the particles has reduced the permanent deformation values of both the subbase and the base samples with an increasing number of F-T cycles up to 5 cycles. The obtained experimental results demonstrate that the hardening and absorption resulting from cement reaction play a significant role in the variation of permanent deformation values, similar to the resilient modulus test. As the number of F-T cycles increases beyond 5 cycles, the permanent deformation values exhibit a slight increase. the permanent deformation values for the base sample show an unexpected increase at 10F-T cycles, reaching 0.0965. Similarly, the subbase sample also experiences an increase in permanent deformation, reaching 0.1116 at 10 cycles. Continuing the analysis, at 20F-T cycles, the permanent deformation values further increased to 0.1060 for the base sample, indicating a 17% increase, and to 0.1295 for the subbase sample, demonstrating a 31% increase when compared to the control samples. This increase in permanent deformation values with increasing F-T cycles can be attributed to the weakening effect of F-T cycles on the RCA. During F-T cycles, the water in the RCA freezes and expands, causing the aggregates to crack and break down, leading to a reduction in the overall strength of the material. This weakening effect results in an increase in permanent deformation values as the number of F-T cycles increases. Moreover, these results indicate that a higher susceptibility to permanent deformation under prolonged F-T exposure and both sample types may exhibit a loss of resistance to deformation beyond a certain threshold of F-T cycles. All the number of F-T, the permanent deformation test results showed that the subbase samples had higher permanent deformation values than the base samples. The base sample's higher gravel content results in less deformation and more stiffness than the subbase. The similar deformation behavior in standard samples is due to variations in particle contact and arrangement.

The findings of this study concerning the effects of F-T cycles on permanent deformation in pavement materials align with previous research in certain aspects. Bozyurt et al. [65], based on results obtained from seven RCA samples collected from different sites, reported that the accumulated permanent deformation values of the RCA samples ranged from 0.5% to 0.8%. In this study, the highest permanent deformation value observed after 20F-T cycles was approximately 0.13%. Li et al. [66] showed the relationship between cumulative permanent strain and the number of F-T cycles in recycled construction waste mixtures. They reported an increase in cumulative permanent strain with increasing F-T cycles, which indicates a reduced susceptibility to deformation.

Moreover, it is essential to consider studies that have reported either no significant influence of F-T cycles on permanent deformation, a significant effect only after a certain threshold of F-T cycles, or different trends altogether. For instance, Soleimanbeigi et al. [55] stated that temperature changes do not significantly impact the permanent deformation values of RCAs and that this effect can generally be ignored. Similarly, Hao et al. [67] argued that only the first four F-T cycles have a major influence and can contribute to an increase in the permanent deformation of crushed waste rocks, which are widely reused in the construction of mine haul roads. Beyond four F-T cycles, the effect of additional cycles was found to be insignificant. Furthermore, Ghorbani

et al. [59] reported unexpected decreases in permanent deformation values for RCA samples as the number of F-T cycles increased. They found that the permanent deformation of RCA, subjected to 0, 10, and 20F-T cycles, decreased after the 10th F-T cycle. The decrease in the permanent deformation of RCA relative to the control sample after 10F-T cycles was 20%. Over the next 10F-T cycles, this decreasing trend was maintained for RCA, resulting in a further 31% decrease in permanent deformation.

In order to gain a better understanding of RCA's behavior, the results from this study were compared with the mechanical behaviors of natural or RCAs studied by other researchers. Wen and Edil [68] reported that the permanent strain for natural Class 6 aggregates was 0.71%. Sebarian and Li [69] examined the permanent deformation properties of natural and recycled aggregates and found that the maximum permanent strain was 0.3745%. Domitrović et al. [70] demonstrated that the results of the permanent deformation test for natural aggregates showed satisfactory repeatability, determined with an average deviation of 12.25%. It was concluded that the RCA used in this study had comparable resistance to permanent deformation as natural aggregates.

3.2. Comparison of resilient modulus models for subbase and base samples

The resilient modulus test results for the sub-base and base samples were evaluated using three different models: Power, Uzan, and MEPD, under various F-T. Fig. 5 displays the resilient modulus test results for these samples, alongside the model constants (k_1, k_2, k_3), coefficient of determination (R^2), and Summary Resilient Modulus (SMR).

In the Power model, it was observed that as the number of F-T cycles increased, the k_1 parameter initially increased, reaching a peak at 5F-T cycles, and then started to decrease. This trend was observed for both base and subbase samples. However, the base samples exhibited a sharper increase in k_1 values compared to the subbase samples. At 5F-T cycles, the base samples reached a peak SMR of 260.16 MPa, while the

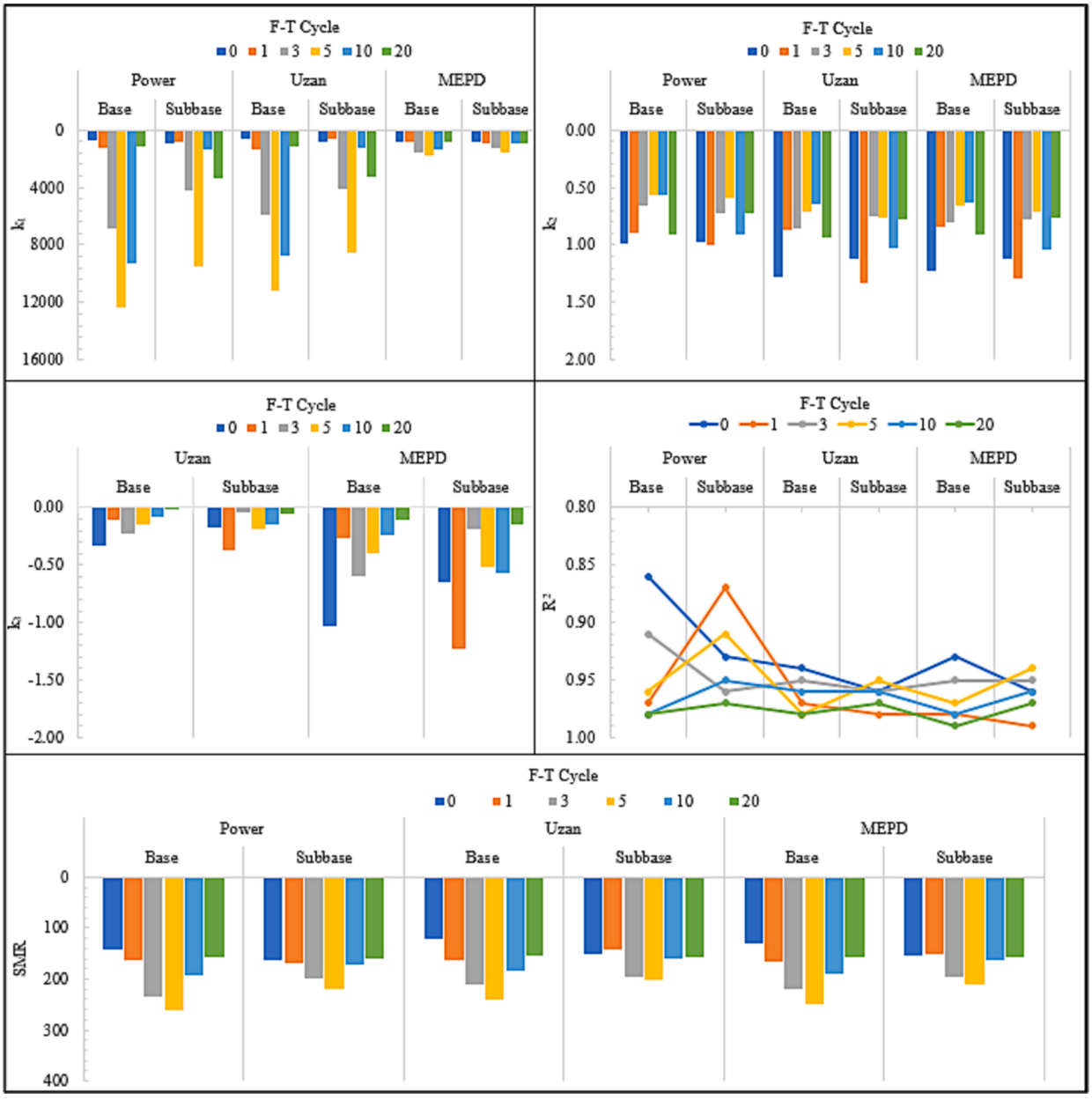

Fig. 5. The change of the model parameters (k1, k2, and k3), as well as the R^2 and SMR values, for the models (Power, Uzan, and MEPD) depending on the number of F-T cycles.

subbase samples peaked at 220.18 MPa. This indicates that the base samples exhibited a higher stiffness and resilience in response to the F-T cycles. Additionally, the k_2 values for both base and subbase samples showed a decrease as the number of F-T cycles increased. However, the decrease was more pronounced for the base samples. This suggests that the base samples experienced a higher degree of stiffness degradation and nonlinear behavior compared to the subbase samples under the influence of F-T cycles. Regarding the Uzan model, similar trends in the k_1, k_2, and k_3 values were observed for both base and subbase samples. The k_1 values showed an increasing trend with the number of F-T cycles, peaking at the 5F-T cycles, with the base samples exhibiting slightly higher peaks than the subbase samples. Furthermore, the k_2 values generally showed a decreasing trend with the increasing number of F-T cycles for both sample types. However, this decrease was more significant for the base samples. As for the k_3 values, they demonstrated minor negative fluctuations for both subbase and base samples in the Uzan model. Conversely, the MEPD model displayed relatively stable k1 values, with a slight increase noticeable at 5F-T cycles for both base and subbase samples. Negative fluctuations were observed in the k_3 values for both sample types. The k_2 parameter, however, demonstrated a higher degree of variability [71,72].

Generally, base samples exhibit higher k_1 values and peak SMR values than the subbase samples, indicating potentially superior resilience. The elevated k_1 values suggest a stiffer response to applied load, indicative of improved material properties and enhanced resistance to deformation. The increased SMR peaks further support this notion, indicating a greater capacity of the material to absorb and dissipate energy during loading. This suggests that the base samples may offer superior resilience to the subbase samples. The pronounced variations in k_2 values among the base samples underline the importance of considering the base material properties and susceptibility to F-T damage when designing and evaluating pavement structures. This may be attributed to the heterogeneous materials used in the base samples and their varied susceptibility to F-T damage. Overall, the models and F-T cycle analysis indicate a good data fit with high R^2 values. Furthermore, earlier research has shown that the advanced correlation parameters of the models selected in this study for estimating resilient modulus have been successful in predicting the resilient modulus of RCAs. For instance, Nokkaew et al. [73] investigated three recycled aggregates with similar gradation. They determined the resilient modulus for each material following the NCHRP 1-28A procedure, finding k_1 values of around 23,500 from the MEPD model, with k_2 and k_3 values of −0.96 and 0.78 respectively. Coban et al. [74] evaluated the long-term performance of coarse and fine recycled aggregate base courses and also used the NCHRP 1-28A procedure to measure the resilient modulus. They found k_1 values from the MEPD model to be between 895 and 930, k_2 values around 0.44, and k_3 values ranging between −0.06 and −0.07. Similarly, Jayakody et al. [75] examined the performance of RCA as a road filling material and utilized the Power, Uzan, and M−EPDG models for estimating the resilient modulus. They confirmed the successful application of these models in predicting the resilient modulus of RCA. For the Uzan model, k_1, k_2, and k_3 values were found to be between 0.6 and 0.7, 0.43 and 0.55, and −0.12 and 0.01 respectively. In the M−EPDG model, k_1, k_2, and k_3 values were found to be between 111 and 127, 0.43 and 0.55, and −0.11 and 0.01 respectively.

Analysis of the models and F-T cycles revealed that R^2 values remained consistently high, all exceeding 0.9. These high R^2 values indicate that the models offer a good fit for the data, implying a strong correlation between predicted and observed values. This suggests that the models are accurate and reliable in capturing the behavior of samples subjected to F-T cycles. Among the various models used for estimating the resilient modulus, the MEPD model showed the best agreement between lab-measured and predicted modulus. Therefore, the MEPD model was chosen for numerical analysis.

3.3. Nonlinear modulus analysis: freeze-thaw & multi-wheel impacts

Prior research has underscored the substantial impact of deep-layer material properties on surface deflection within a multi-course system [76]. This stands in contrast to a homogeneously elastic system where all pavement layers exhibit elastic behavior irrespective of stress–strain conditions. In the predefined sub-coursed system, however, nonlinear properties vary vertically through the course depths within the specified boundaries.

The pavement structure and shoulders were constructed upon the top surface of the roadbed, which is defined as a subgrade assuming infinite soil half-space in the model. The two unbound courses and a flexible bound course of specified materials of designed thickness were placed on the subgrade. The stabilized subbase and base courses consisted of 100% RCA and laid on the natural soil subgrade. The wearing course of the pavement structure was designed as HMA to accommodate the wheel loads [27]. The material properties of the base and subbase courses in the pavement, prior to the F-T cycles, were depicted through an illustration showing the nonlinear change in resilient modulus with depth (as standard properties) in Fig. 6. The modulus of the surface layer was set at 5000 MPa. The initial resilient modulus and its range of variation for the base and subbase layers were established at 2800–200 MPa and 200–40 MPa, respectively. Additionally, the effects of F-T cycles on unbound material properties were tested, and the parameter specifications were established after 1F-T, 3F-T, 5F-T, 10F-T, and 20F-T cycles using the equations of the three models given in Equations 2.1, 2.2, and 2.3. Furthermore, the effects of F-T cycles on unbound material properties were tested and the parameter specification was defined after 1F-T, 3F-T, 5F-T, 10F-T, and 20F-T cycles.

The 3D mechanistic framework of a pavement structure under multiple wheel loads enables the identification of critical failure points through advanced numerical analysis, which are otherwise challenging to discern [77]. Moreover, the time-marching techniques utilized in this research offer the advantage of simultaneously observing the time history of deformations during loading excitation. This contrasts with studies that consider a single wheel load via linearly elastic theory with fundamental axisymmetric assumptions. The conducted analysis investigates deformations varying both horizontally within each course and vertically through the thickness of the courses [78].

The results of the research on mechanistic response models can be categorized into three main parts: (1) Comparing the effects of the nonlinear resilient modulus as determined by the Mechanistic-Empirical Pavement Design (MEPD), Hicks and Monismith (power model), and Uzan Model on the permanent deformation of pavement courses, (2) Evaluating the performance of pavement designed with recycled concrete aggregate under F-T cycles, (3) Investigating critical pavement responses under multiple wheel loads by determining the most extreme values (stress, strain, and displacements) at various depths and locations within the 3D flexible pavement model.

Unstable pavement courses can often undergo permanent deformation, primarily beneath wheel tracks. While rutting on the surface can be attributed to various layers, research, such as the AASHO road testing, indicates the significant contribution from both surface courses and underlying layers. In other words, the geotechnical conditions of the unbound materials throughout the pavement can result in a much broader rut due to deep-seated deformations [34]. Thus, in evaluating pavement performance, the longitudinal depression of the pavement under wheel paths, also known as rutting, is taken into account and compared to the limits in design codes. In this study, the criteria outlined by the current version of the NCHRP 1-37A design method are considered.

The graph depicted in Fig. 7 shows the maximum deformation values recorded along the A-A and B-B sections, which are parallel to the traffic direction. The results of the analyses conducted using the material properties determined before the F-T cycle have been compared. These properties were evaluated using the MEPD, Uzan, and Power models.

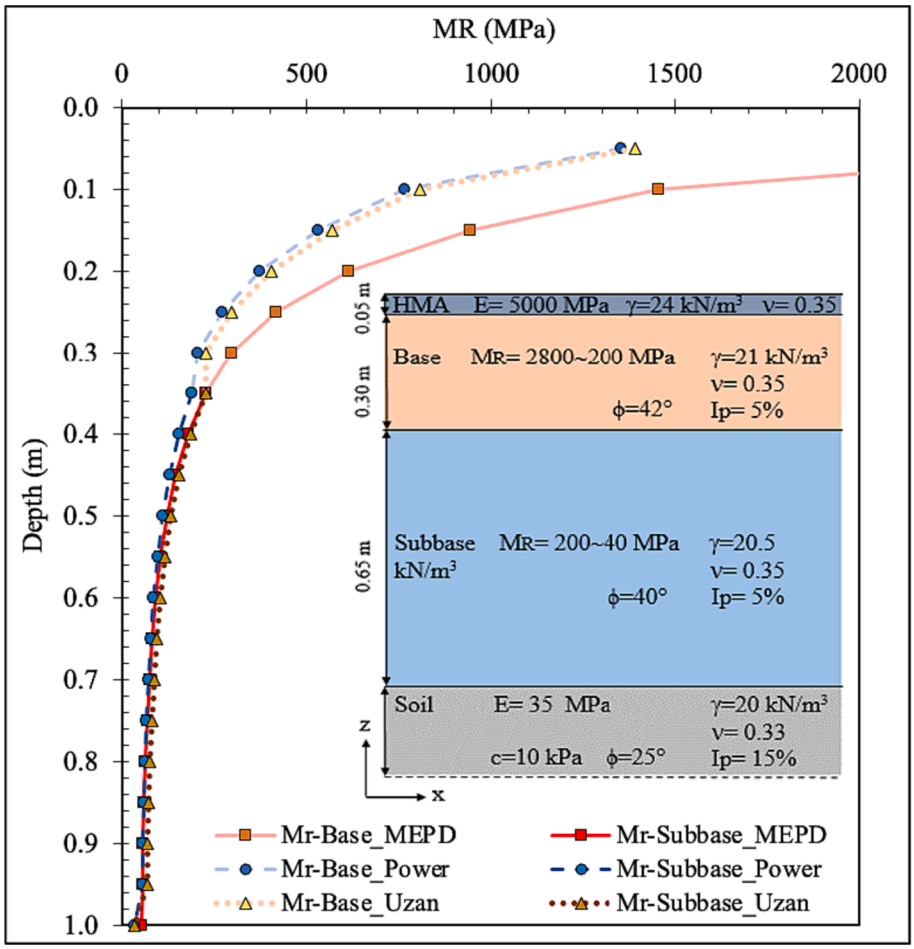

Fig. 6. Material properties of the pavement and resilient modulus before F-T cycles.

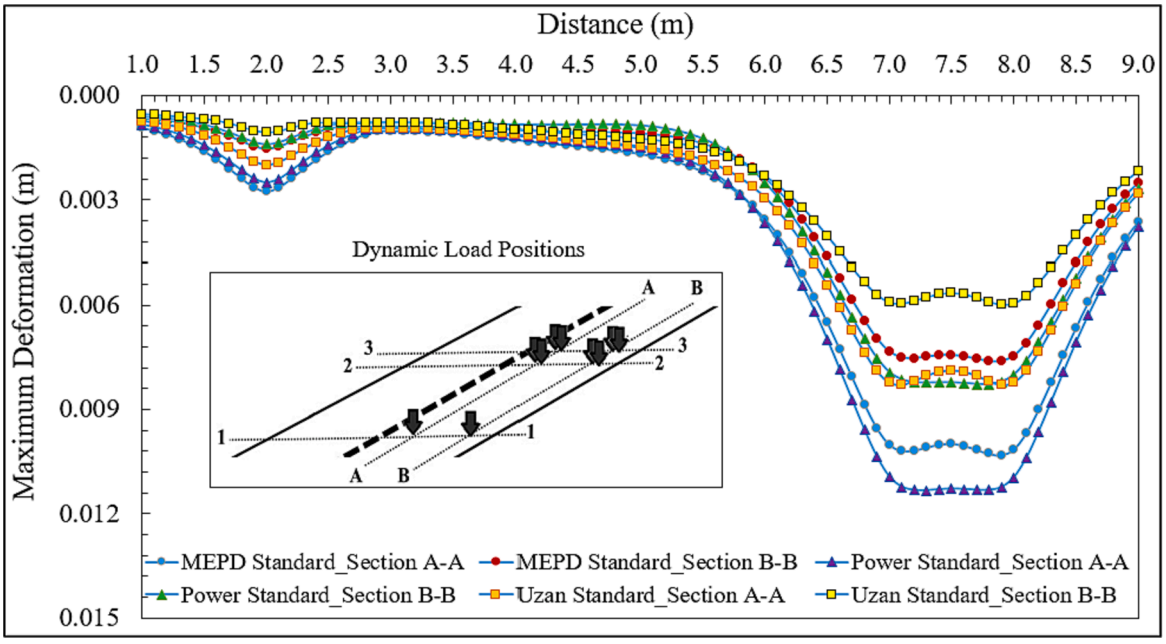

Fig. 7. Longitudinal maximum deformations beneath the wheel tracks.

The observed values of the largest deformations, measured directly beneath the front axle at section 1-1 in the pavement, ranged from 1 × 10^{-3} m to 2.5 × 10^{-3} m. The smallest value under the tandem load was recorded as 6 × 10^{-3} m using the Uzan model. Conversely, the Power model resulted in the largest deformation value of 11 × 10^{-3} m in the A-A section and 8.3 × 10^{-3} m in the B-B section on the axis 3–3.

However, for the 2–2 and 3–3 axles, the maximum deformations recorded along the A-A axis are significantly higher than the values noted along the B-B axis, which is closer to the edge of the slope. This finding could indicate a potential internal failure plane within the slope of the pavement structure. Thus, the results of the analysis clearly underscore the necessity of performing assessments under multiple loads

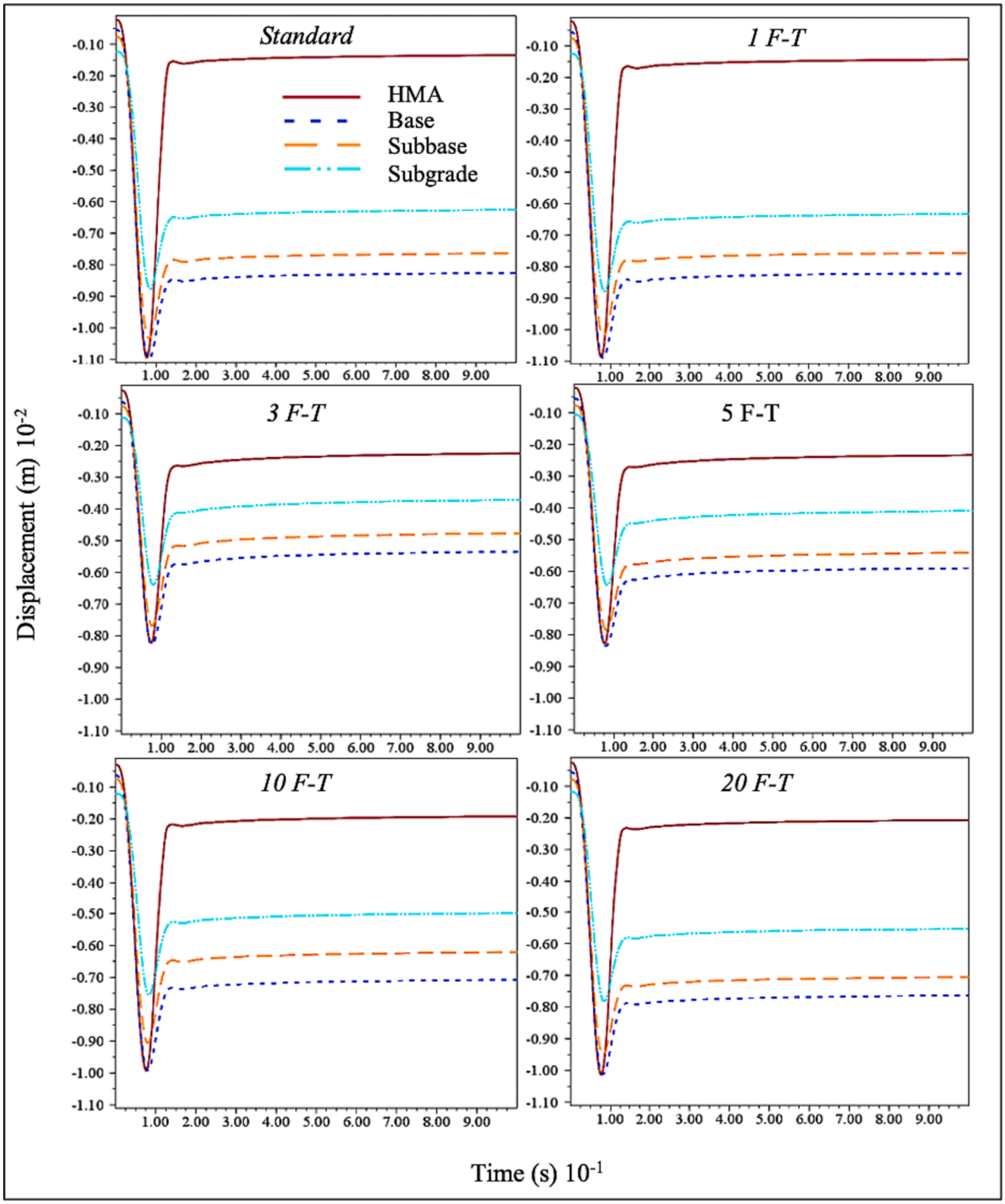

Fig. 8. The maximum displacement time history at the top of the 3-A position for each course, following F-T cycles, was examined across Power model.

within a three-dimensional, real-world geometric context.

Moreover, there are limited research provide evidence and support for the statement that the 3D mechanistic framework enables the identification of failure points and the observation of deformations in pavement structures under multiple loads. For example, Wang & Ma [79] highlighted the heightened deformation in base asphalt pavements due to varying factors. Similarly, findings from Manuka & Lachore [80] and Bai & Zhang [81] underscore the influence of different distress forms and material property variations on pavement behavior.

3.4. Evaluation of the RCA performance under F-T cycles

The maximum displacement time histories at the top of HMA, base, subbase, and subgrade courses, post various F-T cycles, have been illustrated for three models under wheel set 3-A in Figs. 8–10. In the MEPD model, following the 5F-T cycle, a decrease in the permanent

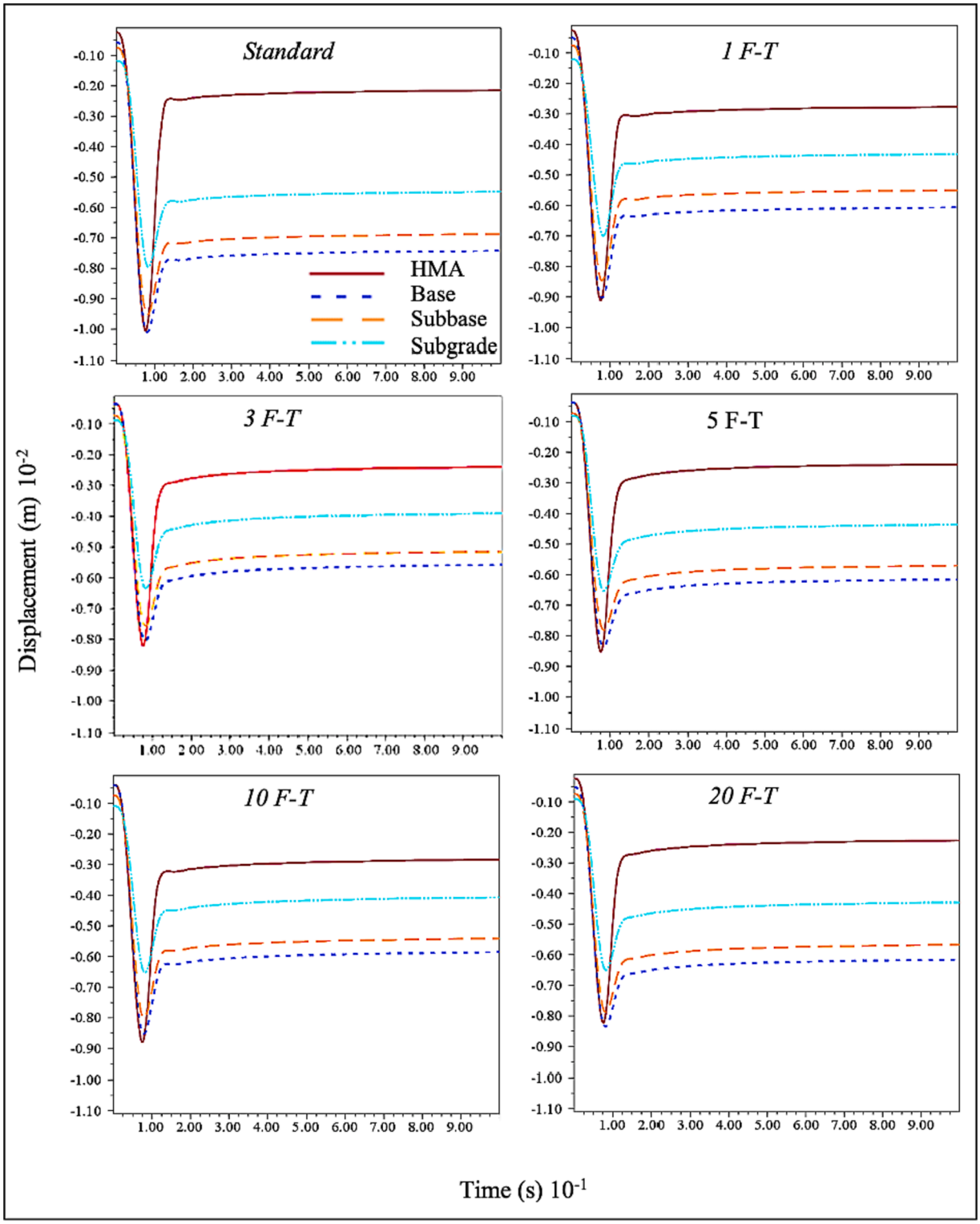

Fig. 9. The maximum displacement time history at the top of the 3-A position for each course, following F-T cycles, was examined across Uzan model.

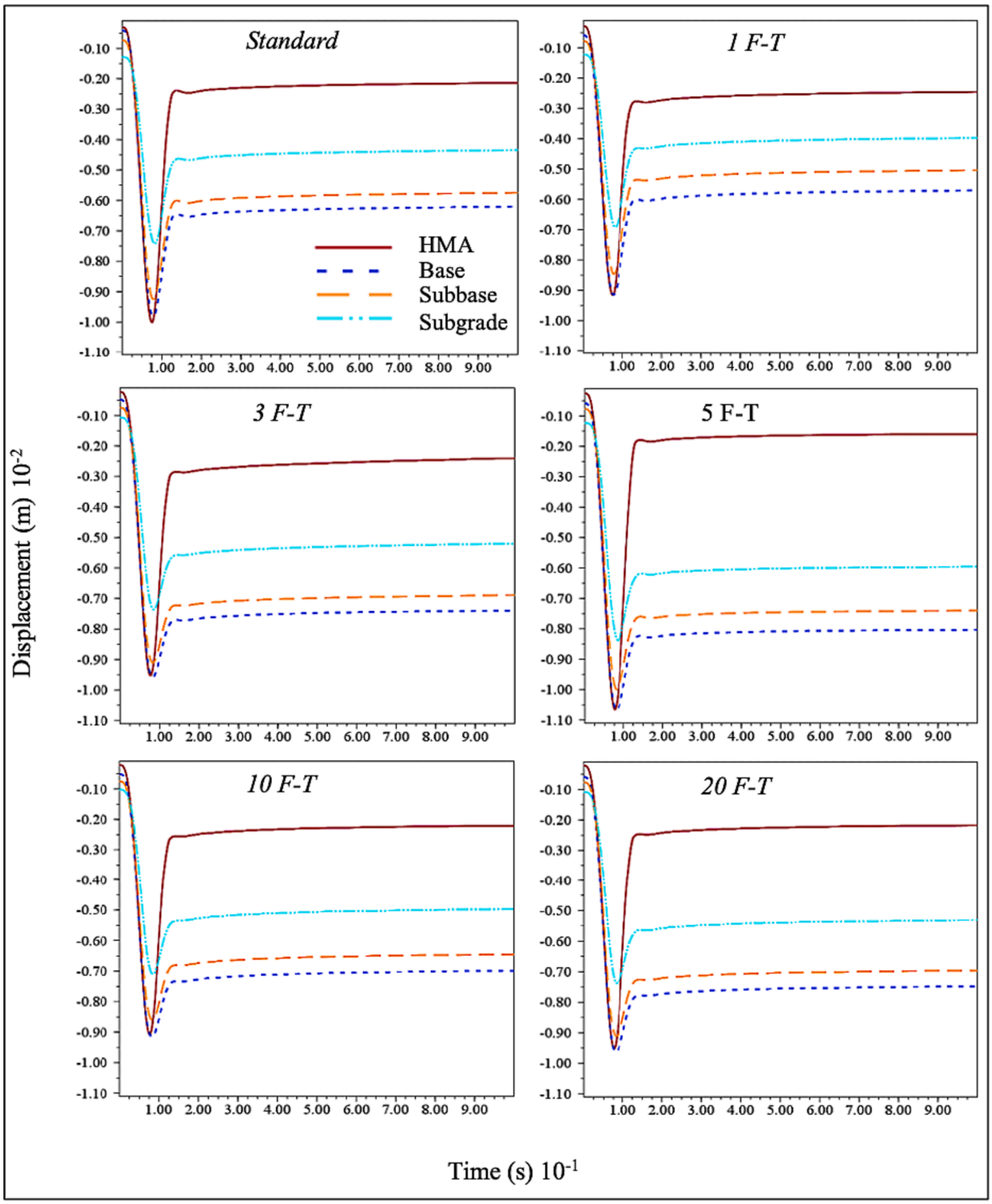

Fig. 10. The maximum displacement time history at the top of the 3-A position for each course, following F-T cycles, was examined across MEPD model.

deformation value in the HMA course was noted, while an increase was observed in the other sub-courses. Moreover, the change of the displacement with depth at the top of the 3-A position following F-T cycles, was examined across the models were given in Figs. 11–13.

As seen in Figs. 8–13, the material properties of the courses, which were calculated with the nonlinear resilient modulus coefficients, induce the largest displacement after the 5F-T cycle in analyses using the MEPD model. Conversely, following the 5 and 10F-T cycles in the Uzan model, it is evident that the largest and permanent displacements of the sub courses gradually decrease, while the permanent deformation of the HMA on the surface rises. In the results obtained from the Power model, a significant decrease in displacements is observed after the fifth cycle, followed by an increase in the sub courses' values in subsequent cycles. Moreover, it's notable that the curves representing the permanent displacements occurring on the surface of the HMA course and the sub courses under standard conditions in the MEPD models closely align with each other. The smaller disparity between the lower group and the top course, compared to other models, is a significant indication that deformations are more uniformly distributed among the courses. Moreover, as F-T cycles increase, it can be inferred that the courses

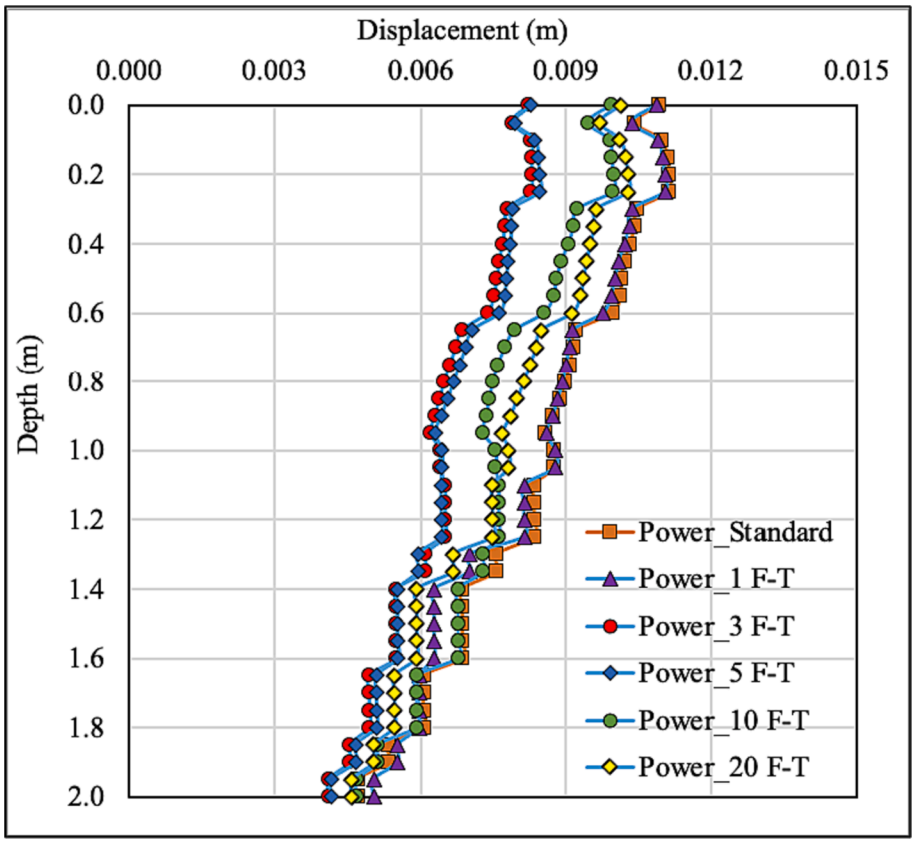

Fig. 11. The change of the displacement with depth at the top of the 3-A position following F-T cycles, was examined across Power model.

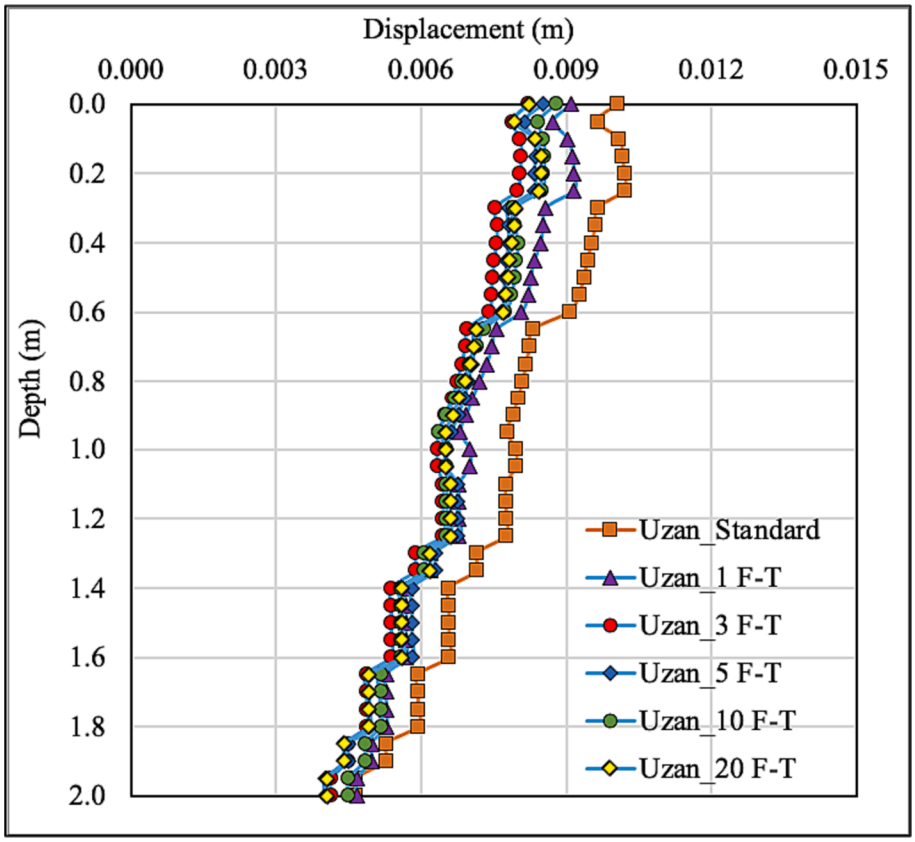

Fig. 12. The change of the displacement with depth at the top of the 3-A position following F-T cycles, was examined across Uzan model.

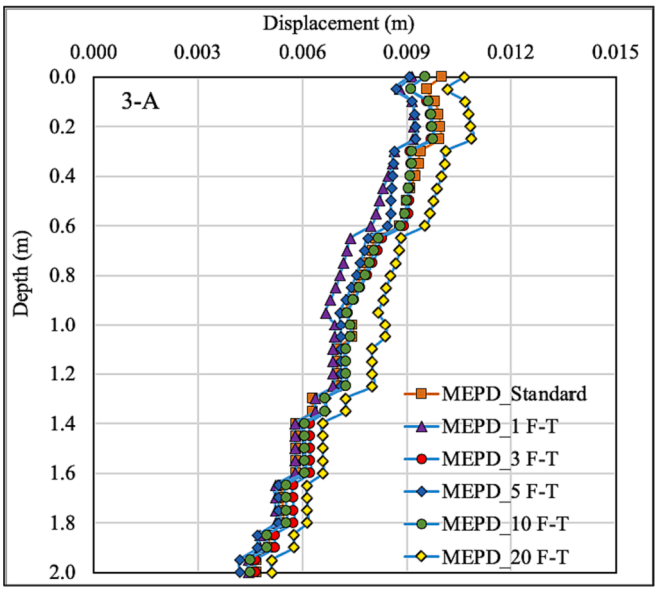

Fig. 13. The change of the displacement with depth at the top of the 3-A position following F-T cycles, was examined across MEPD model.

defined by the Uzan model distribute deformations in a more balanced manner.

This was executed to study the alterations in material specifications subjected to diverse environmental circumstances. Concurrently, the permanent deformations for each model impart valuable insights regarding the performance of the RCA in base and subbase courses under F- T conditions. The permanent deformations observed at the top of each course, under the material conditions ascertained for the initial state and after 20F-T cycles, are presented in Fig. 14.

Upon examining the values measured under the maximum deformation, we notice a decrease in the rutting value on top of the HMA course of the MEPD model from 2.14 × 10^{-3} m to 1.60 × 10^{-3} m over long-term F-T behavior. However, examining the values observed in the lower courses reveals a significant increase in the permanent deformation value in the base, from 6.20 × 10^{-3} m to 8 × 10^{-3} m, in the subbase course from 5.75 × 10^{-3} m to 7.40 × 10^{-3} m, and in the subgrade course from 4.35 × 10^{-3} m to 5.95 × 10^{-3} m. This can be attributed to the phenomenon where the cover course separates from the lower courses after F-T cycles, leading to reduced rutting on the surface [82,83].

The 3D numerical analyses presented in Fig. 15 demonstrate the total permanent deformations observed for the standard subbase and base courses, as well as those subjected to 20F-T cycles. This figure indicates that the obtained permanent deformations are slightly higher than the laboratory results, as seen when comparing Fig. 5(a). In contrast to the rutting decrease on the surface, the increase in total settlement at the bottom courses negatively impacts pavement performance. This could result in the failure of the HMA course due to the concentration of tensile strain on the uncontacted base-HMA interface (at the bottom of HMA) through a narrow rut [84–86]. The maximum rutting observed in the pavement is lower than the standard values of 11.51 mm and 19.05 mm, as specified respectively in the AASHTO Guide for Design of Pavement Structures [78] and NCHRP 1-37A [32].

3.5. *Investigation of the critical pavement responses in 3D numerical models*

The vertical displacements before the 1F-T cycle and after the 20F-T cycle in the pavement model constructed by MEPD are depicted in Fig. 16. Upon examining the color shading of the 3D Finite Difference Model, it's apparent that the HMA course conveys the loads via flexible behavior. The gradual attenuation of displacement in the vertical direction can be monitored by observing the shading circles.

Multiple loads resulted in maximum vertical displacements, initially reaching 6.50 × 10^{-3} m, which increased by 25% to 8.35 × 10^{-3} m after 20F-T cycle. Furthermore, by examining the turquoise-colored shadings underneath the pavement throughout the model, it is suggested that the displacement in the subgrade is greater than in the base and subbase courses. In conclusion, the strength degradation of geomaterials caused by F-T cycles may lead to excessive deformation and inherent failures. Inadequate base and subbase materials can exacerbate this degradation [87–89].

4. Conclusion

This study investigated the potential of utilizing recycled concrete aggregates (RCA) in the development of high-performance and durable flexible pavements. The paper focused on the effects of freeze–thaw (F-T) cycles on the stiffness properties of subbase and base samples prepared with RCA. Resilience modulus and permanent deformation tests were conducted under freeze–thaw conditions to ascertain the stiffness characteristics of these samples. The parameters obtained from these laboratory tests were then used in a 3D nonlinear numerical analysis, under similar conditions, to determine the cumulative plastic deformation (rutting) of the pavement courses and the maximum deflection values under multiple wheel loads.

The laboratory tests conducted on RCA samples indicated that their stiffness properties met the required specifications for subbase and base materials, demonstrating their potential for use in flexible pavement construction. The resilient modulus and permanent deformation values

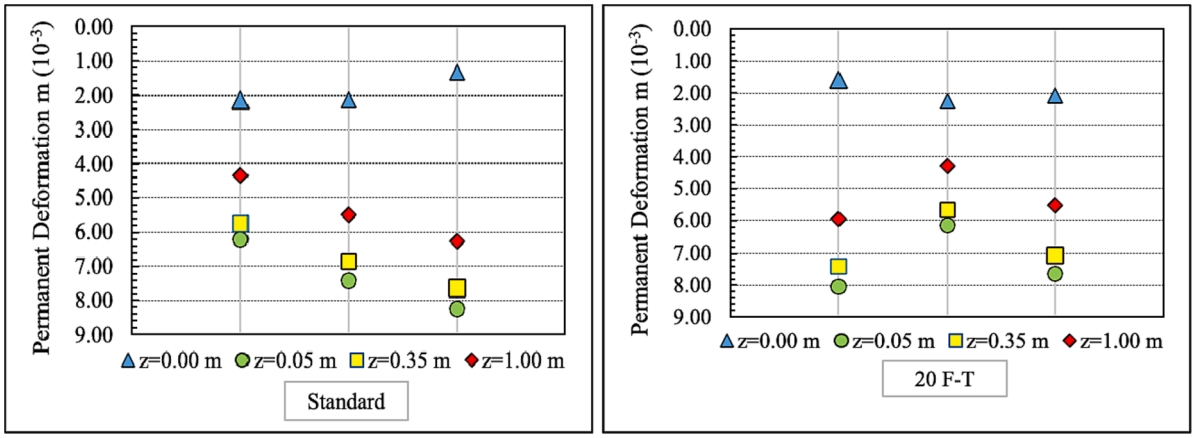

Fig. 14. Permanent deformations for each model under the point of observed maximum surface distress.

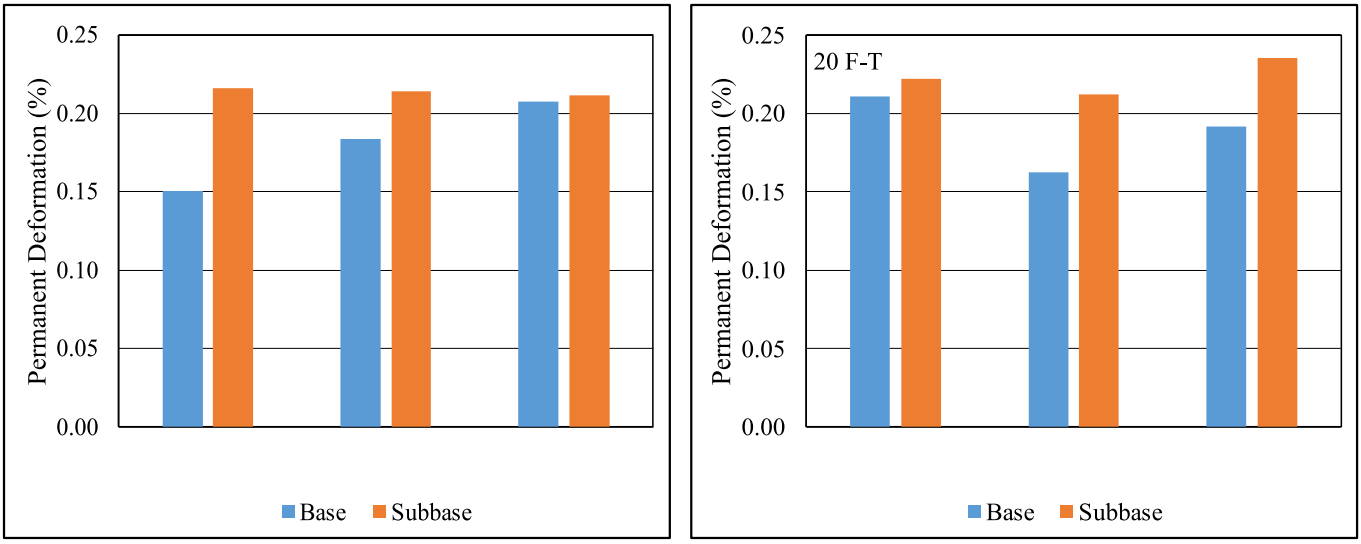

Fig. 15. Permanent deformations observed for the standard subbase and base courses, as well as those subjected to 20F-T cycles.

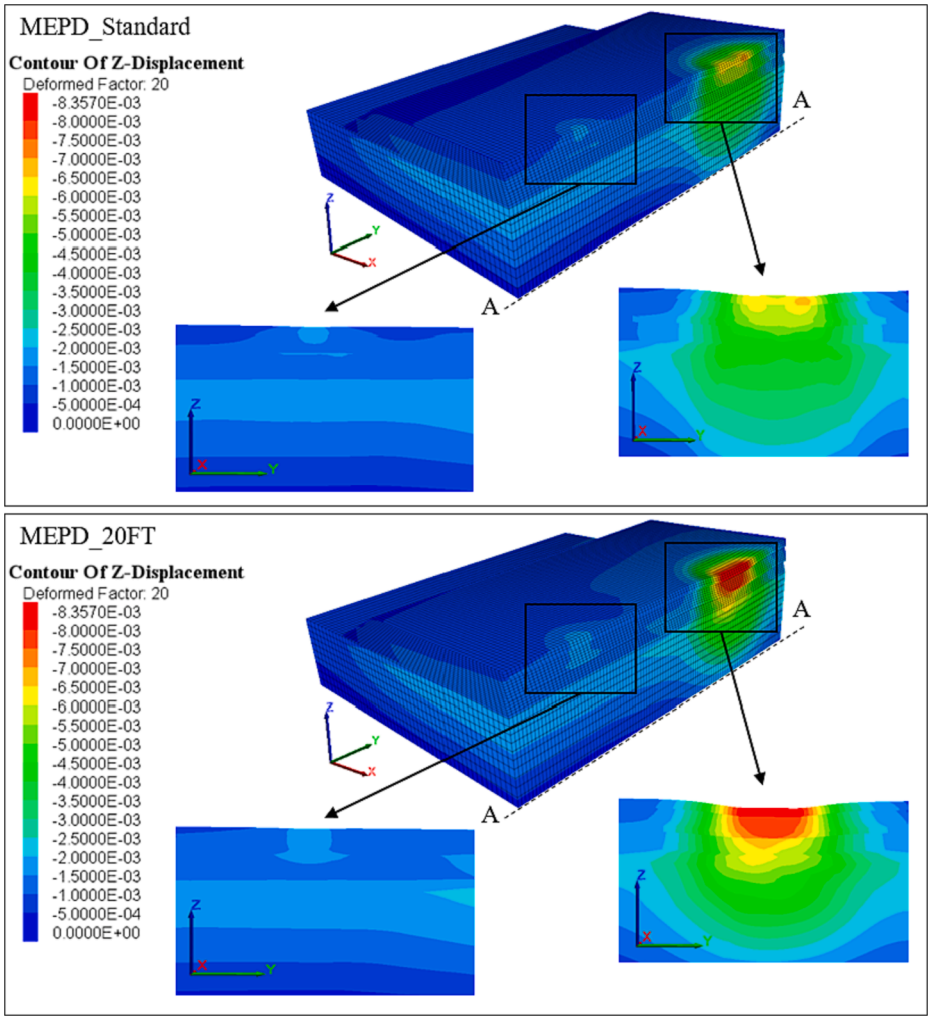

Fig. 16. Contour of z-displacement for MEPD material models at initial condition and after 20F-T cycles.

initially increased up to a certain number of F-T cycles, attributed to the cementing effect of fine particles and partial densification. However, continued exposure to F-T cycles resulted in a decline in the resilient modulus, indicating a weakening of the samples' internal structure. A comparison of three different resilient modulus models (MEPD, Power, and Uzan) illustrated variations in the distribution of permanent

deformation among pavement courses. The MEPD model demonstrated a more uniform distribution, while the Uzan model exhibited a more balanced distribution under F-T conditions. These models, along with the numerical analysis conducted, provided valuable insights into the behavior of pavement structures under multiple wheel loads and F-T conditions.

The numerical analysis indicated that the HMA course exhibited flexible behavior, transmitting loads through a gradual attenuation of vertical displacement. The degradation of geomaterial strength due to F-T cycles resulted in excessive deformation, particularly in the subgrade. This underlines the importance of considering the quality of base and subbase materials in RCA-based pavements to mitigate deformation and potential failures. Notably, the total rutting values obtained in this study are satisfactory according to relevant standards.

The results suggest that RCA has potential for use in pavement structures, exhibiting effective stiffness performance and rutting resistance. However, it's important to note that this material is sensitive to temperature fluctuations, and the content of recycled material should be carefully determined through detailed investigation during the optimization of mixture design. The use of RCA can contribute to sustainable and environmentally friendly pavement solutions, but it requires careful consideration of its properties and behavior under F-T conditions.

This study lays the groundwork for subsequent investigations on RCA and its potential implications on modern infrastructural developments. The findings underscore the importance of not just identifying sustainable materials but also thoroughly understanding their behavior under diverse operational conditions. However, this research mainly concentrated on the behavior of RCA under F-T conditions. Future research can delve deeper into understanding RCA's performance under varied climatic conditions, drainage factor in overall pavement performance, load frequencies, and long-term aging. Additionally, a comparative study involving RCA and other recycled materials could offer a clearer picture of the most viable options for sustainable pavements.

Declaration of Competing Interest

The authors declare that they have no known competing financial interests or personal relationships that could have appeared to influence the work reported in this paper.

Data availability

Data will be made available on request.

References

[1] Mohammadinia, A., Arulrajah, A., Sanjayan, J., Disfani, M. M., Bo, M. W., & Darmawan, S. (2015). Geotechnical properties of lightly stabilized recycled demolition materials in base/sub-base applications. In IFCEE 2015 (pp. 2767-2776).

[2] Q. Tang, P. Xiao, C. Kou, K. Lou, A. Kang, Z. Wu, Physical, chemical and interfacial properties of modified recycled concrete aggregates for asphalt mixtures: A review, Constr. Build. Mater. 312 (2021), 125357.

[3] X. Xu, Y. Luo, A. Sreeram, Q. Wu, G. Chen, S. Cheng, X. Chen, Potential use of recycled concrete aggregate (RCA) for sustainable asphalt pavements of the future: A state-of-the-art review, J. Clean. Prod. 130893 (2022).

[4] H. Khandelwal, H. Dhar, A.K. Thalla, S. Kumar, Application of life cycle assessment in municipal solid waste management: A worldwide critical review, J. Clean. Prod. 209 (2019) 630–654.

[5] R. Cardoso, R.V. Silva, J. de Brito, R. Dhir, Use of recycled aggregates from construction and demolition waste in geotechnical applications: A literature review, Waste Manag. 49 (2016) 131–145.

[6] H.S. Coban, B. Cetin, T.B. Edil, Q. Sun, Evaluation of Mechanical Degradation Characteristics of Recycled and Natural Aggregates Under Gyratory Compaction Effort, Transp. Geotech. 100743 (2022).

[7] Cetin, B., Gheibi, I., Edil, T. B., Hatipoglu, M., & Coban, H. S. (2021). Improve Material Inputs into Mechanistic Design Properties for Reclaimed HMA & Recycled Concrete Aggregate (RCA) Roadways (No. NRRA202105). Minnesota. Department of Transportation.

[8] L.S.P. Gopisetti, H. Ceylan, S. Kim, B. Cetin, O. Kaya, Sensitivity Index Comparison of Pavement Mechanistic-Empirical Design Input Variables to Reflect Cracking Model for Different Climatic Zones, Road Mater. Pavement Design (2020) 1–16.

[9] L.S.P. Gopisetti, B. Cetin, B. Forman, S. Durham, C. Schwartz, H. Ceylan, Evaluation of Four Different Climate Sources on Pavement Mechanistic-Empirical Design and Impact of Surface Shortwave Radiation, Int. J. Pavement Eng. (2019) 1–14.

[10] Q. Li, X. Ling, Sheng D, Elasto-plastic behaviour of frozen soil subjected to long-term low-level repeated loading, Part I: Experimental investigation, Cold Reg. Sci. Technol. 125 (2016) 138–151.

[11] M.G. Rosa, B. Cetin, T.B. Edil, C.H. Benson, Freeze-thaw performance of fly ash-stabilized materials and recycled pavement materials, J. Mater. Civ. Eng. 29 (6) (2017) 04017015.

[12] M. Bassani, L. Tefa, Compaction and freeze-thaw degradation assessment of recycled aggregates from unseparated construction and demolition waste, Constr. Build. Mater. 160 (2018) 180–195.

[13] Ovad, E., Barišić, I., Zagvozda, M. (2014). Comparison Of Croatian and European Standards For Determining The Frost Susceptibility Of Hydraulically Bound Mixtures. e-GFOS, 41-48. https://doi.org/10.13167/2014.9.5.

[14] B. Likar, S. Lenart, K. Bizjak, A. Tang, Experiences From In-situ Monitoring Of Pavement Under Weather Conditions Change, E3S Web Conf. 9 (2016) 20003, https://doi.org/10.1051/e3sconf/20160920003.

[15] T. Kumela, Evaluation Of Flexible Pavement Deflections With Respect To Pavement Depths Using Software (A Case Study Jimma To Seka Road), AJCE 5 (6) (2018) 141. https://doi.org/10.11648/j.ajce.20180605.11.

[16] M. Khabiri, B. Ebrahimialavijeh, Effect Of Freezing and Thawing On The Strength And Durability Of Sandy Subgrade Containing Fibrillating Network Fiber For Pavement, CEJ 2 (29) (2020). https://doi.org/10.14311/cej.2020.01.0014.

[17] T. Liao, I. Kumar, M.S. Dojutrek, S. Labi, Updating Secondary Climate Attributes For Transportation Infrastructure Management, J. Infrastruct. Syst. 1 (24) (2018), https://doi.org/10.1061/(asce)is.1943-555x.0000396.

[18] W. Wang, Y. Cheng, G. Ma, G. Tan, X. Sun, S. Yang, Further Investigation On Damage Model Of Eco-friendly Basalt Fiber Modified Asphalt Mixture Under Freeze-thaw Cycles, Appl. Sci. 1 (9) (2018) 60, https://doi.org/10.3390/app9010060.

[19] J. Bilodeau, G. Doré, Assessment Of Pavement Response During Spring Thaw Using Heavy Vehicle Simulator Testing, J. Test. Eval. 1 (48) (2019) 20180921, https://doi.org/10.1520/jte20180921.

[20] Z. Ye, Y. Lu, L. Wang, Investigating the Pavement Vibration Response For Roadway Service Condition Evaluation, Adv. Civil Eng. 2018 (2018) 1–14, https://doi.org/10.1155/2018/2714657.

[21] Bonger, A., Hosoda, A., Salem, H., Fukaya, T. (2022). Numerical Simulation Of Rupture and Protrusion Of Vertically Tightened Pc Bars In Pc Girders With Asphalt Pavement Using Applied Element Method. Journal of JSCE, 1(10), 145-161. https://doi.org/10.2208/journalofjsce.10.1_145.

[22] Z. Cao, N. Liang, S. Zeng, X. Gang, Development Of a Continuous Testing Device For Pavement Structure Bearing Capacity, Processes 11 (10) (2022) 2325, https://doi.org/10.3390/pr10112325.

[23] D. Kim, A. Norouzi, S. Kass, T. Liske, Y.R. Kim, Mechanistic performance evaluation of pavement sections containing RAP and WMA additives in Manitoba, Constr. Build. Mater. 133 (2017) 39–50, https://doi.org/10.1016/j.conbuildmat.2016.12.035.

[24] D. Moazami, A. Sahaf, A.M. Moghaddam, Investigating the Rutting Behavior of Modified Asphalt Mixtures with Waste Materials, Numer. Methods Civil Eng. 3 (4) (2019) 53–65.

[25] A. Mohammadinia, A. Arulrajah, M. M. Disfani, S. Darmawan, Small-Strain Behavior of Cement-Stabilized Recycled Concrete Aggregate in Pavement Base Layers, 31 (5) (2019) 1–13.

[26] I. Pérez, L. Medina, B. Gómez-Meijide, P.A. Costa, A.S. Cardoso, Numerical simulation of bitumen emulsion-stabilised base course mixtures with C&D waste aggregates considering nonlinear elastic behaviour, Constr. Build. Mater. 249 (2020), 118696, https://doi.org/10.1016/j.conbuildmat.2020.118696.

[27] M. Akbas, B. Özaslan, H. Khanbabazadeh, R. İyisan, Numerical study using stiffness parameters on the nonlinear behavior of rca pavements under heavy traffic loads, Transp. Geotech. 29 (2021), 100582.

[28] AASHTO, Guide for Design of Pavement Structures American Association of State Highway and Transportation Officials (AASHTO), Washington D.C., 1993.

[29] AASHTO T307-99, Determining the resilient modulus of soils and aggregate materials. American Association of State Highway and Transportation Officials (AASHTO), Washington D.C., 2007.AASHTO *Pavement* Structures Design Guidelines.

[30] R.G. Hicks, Factors influencing the resilient response of granular materials, University of California, Berkeley, USA, 1970. Doctoral Dissertation.

[31] J. Uzan, M.W. Witczak, T. Scullion, R.L. Lytton, Development and validation of realistic pavement response models, in: 7th International Conference on Asphalt Pavements, Nottingham, UK, 1992, pp. 334–350.

[32] NCHRP (National Cooperative Highway Research Program), Guide for Mechanistic-Empirical Design of New and Rehabilitated Pavement Structures, Part 2 Design Inputs, Final Report NCHRP 1-37A, 2004.

[33] Christopher, B. R., Schwartz, C. And Boudreau, R. (2006). Geotechnical Aspects of Pavements, Federal Highway Administration, no. 132040.

[34] S. Cho, C. Tóth, Z. Soós, Finite Element Method analysis for mechanistic design in flexible pavement, Review: From how to build a material in FE analysis to complexity in reality, Epa, - J. Silic. Based Compos. Mater. 70 (6) (2018) 204–208.

[35] D.H. Chen, M. Zaman, J. Laguros, A. Soltani, Assessment of computer programs for analysis of flexible pavement structure, Transp. Res. Rec. 1482 (137) (1995) 123–133.

[36] E. Heymsfield, J.S. Tingle, State of the practice in pavement structural design/analysis codes relevant to airfield pavement design, Eng. Fail. Anal. 105 (June 2018) (2019) 12–24, https://doi.org/10.1016/j.engfailanal.2019.06.029.
[37] Itasca Consulting Group, FLAC3D Manual- Fast Lagrangian Analysis of Continua in Three-Dimensions, Minneapolis; 2017.
[38] Ozaslan, B., Iyisan, R., Hasal, M. E., Khanbabazadeh, H., & Yamanaka, H. (2021). Assessment of the Design Spectrum with Aggravation Factors by 2D Nonlinear Numerical Analyses: A Case Study in Gemlik Basin, Turkey. Bulletin of Earthquake Engineering, (0123456789), 0–3. https://doi.org/10.1007/s10518-021-01296-6.
[39] I. Ishibashi, X. Zhang, Unified Dynamic Shear Moduli and Damping Ratios of Sand and Clay, Soils Found. 33 (1) (1993) 182–191.
[40] "Estimating Cumulative Traffic Loads, Volume II : Traffic Data Assessment and Axle Load Projection for the Sites with Acceptable Axle Weight Data, Final Report for Phase 2," vol. II, no. March, 2005.
[41] B. Ghorbani, E. Yaghoubi, A. Arulrajah, S. Fragomeni, Long-Term Performance Analysis of Demolition Waste Blends in Pavement Bases Using Experimental and Machine Learning Techniques, Int. J. Geomech. 23 (6) (2023) 04023058.
[42] D. Mishra, E. Tutumluer, Aggregate physical properties affecting modulus and deformation characteristics of unsurfaced pavements, J. Mater. Civ. Eng. 24 (9) (2012) 1144–1152.
[43] Y. Xiao, K. Kong, U.F. Aminu, Z. Li, Q. Li, H. Zhu, D. Cai, Characterizing and Predicting the Resilient Modulus of Recycled Aggregates from Building Demolition Waste with Breakage-Induced Gradation Variation, Materials 15 (7) (2022) 2670.
[44] B. Ghorbani, E. Yaghoubi, A. Arulrajah, Thermal and mechanical characteristics of recycled concrete aggregates mixed with plastic wastes: experimental investigation and mathematical modeling, Acta Geotech. 17 (7) (2022) 3017–3032.
[45] H.S. Coban, B. Cetin, H. Ceylan, T.B. Edil, W.J. Likos, Evaluation of Engineering Properties of Recycled Aggregates and Preliminary Performance of Recycled Aggregate Base Layers, J. Mater. Civ. Eng. 34 (5) (2022) 04022053.
[46] M.R. Kaloop, A.R. Gabr, S.M. El-Badawy, A. Arisha, S. Shwally, J.W. Hu, Predicting resilient modulus of recycled concrete and clay masonry blends for pavement applications using soft computing techniques, Front. Struct. Civ. Eng. 13 (2019) 1379–1392, https://doi.org/10.1007/s11709-019-0562-2.
[47] E. Yaghoubi, N. Sudarsanan, A. Arulrajah, Stress-strain response analysis of demolition wastes as aggregate base course of pavements, Transp. Geotech. 30 (2021), 100599.
[48] Cancino, P. (2023). laboratory study of durability of recycled concrete aggregate including drainage for use in pavement base course.
[49] E.B. Toka, M. Olgun, Performance of granular road base and sub-base layers containing recycled concrete aggregate in different ratios, Int. J. Pavement Eng. 23 (11) (2023) 3729–3742.
[50] Bozyurt, O., Keene, A.K., Tinjum, J.M., Edil, T.B., Fratta, D. (2013). Freeze–Thaw Effects on Stiffness of Unbound Recycled Road Base, Mechanical Properties of Frozen Soil, PA: ASTM International, 3-21.
[51] Monu, K., RN, G. R., Pandey, G. S., & Singh, S. (2020). Performance evaluation of recycled-concrete aggregates and reclaimed-asphalt pavements for foam-mix asphalt mixes. Journal of Materials in Civil Engineering, 32(10), 04020295.
[52] B. Ghorbani, A. Arulrajah, G. Narsilio, S. Horpibulsuk, M. Leong, Resilient moduli of demolition wastes in geothermal pavements: Experimental testing and ANFIS modelling, Transp. Geotech. 29 (2021), 100592.
[53] Z. Zhou, W. Ma, S. Zhang, Y. Mu, G. Li, Effect of freeze-thaw cycles in mechanical behaviors of frozen loess, Cold Reg. Sci. Technol. 146 (2018) 9–18.
[54] Z. Wei, W. Yang, C. Zhai, Y. Sun, W. Tang, A. Chen, Y. Wang, Freezing characteristics and microstructural damage evolution of granular materials in cold regions under freezing–thawing cycles, Environ. Earth Sci. 82 (7) (2023) 1–17.
[55] A. Soleimanbeigi, R.F. Shedivy, J.M. Tinjum, T.B. Edil, Climatic effect on resilient modulus of recycled unbound aggregates, Road Mater. Pavement Design 16 (4) (2015) 836–853.
[56] M.G. Rosa, B. Cetin, T.B. Edil, C.H. Benson, Freeze–thaw performance of fly ash–stabilized materials and recycled pavement materials, J. Mater. Civ. Eng. 29 (6) (2017) 04017015.
[57] J. Zhang, A. Zhang, C. Huang, H. Yu, C. Zhou, Characterising the resilient behaviour of pavement subgrade with construction and demolition waste under Freeze-Thaw cycles, J. Clean. Prod. 300 (2021), 126702.
[58] M. Diagne, J.M. Tinjum, K. Nokkaew, The effects of recycled clay brick content on the engineering properties, weathering durability, and resilient modulus of recycled concrete aggregate, Transp. Geotech. 3 (2015) 15–23.
[59] B. Ghorbani, A. Arulrajah, G. Narsilio, S. Horpibulsuk, Experimental investigation and modelling the deformation properties of demolition wastes subjected to freeze–thaw cycles using ANN and SVR, Constr. Build. Mater. 258 (2020), 119688.
[60] H.H. Titi, M.G. Matar, Estimating resilient modulus of base aggregates for mechanistic-empirical pavement design and performance evaluation, Transp. Geotech. 17 (2018) 141–153.
[61] M. Arshad, M.F. Ahmed, Potential use of reclaimed asphalt pavement and recycled concrete aggregate in base/subbase layers of flexible pavements, Constr. Build. Mater. 151 (2017) 83–97.
[62] M. Arisha, A., Gabr, A. R., El-Badawy, S. M., & Shwally, S. A. (2018). Performance evaluation of construction and demolition waste materials for pavement construction in Egypt. Journal of Materials in Civil Engineering, 30(2), 04017270.
[63] Y. Zhang, B. Cetin, T.B. Edil, Seasonal Performance Evaluation of Pavement Base Using Recycled Materials, Sustainability 13 (22) (2021) 12714.
[64] Cavalline, T. L., Snyder, M. B., & Taylor, P. (2022). Use of Recycled Concrete Aggregate (RCA) in Concrete Paving Mixtures [tech brief] (No. FHWA-HIF-22-020). United States. Federal Highway Administration.
[65] O. Bozyurt, J.M. Tinjum, Y.-H. Son, T.B. Edil, C.H. Benson, Resilient Modulus of Recycled Asphalt Pavement and Recycled Concrete Aggregate, GeoCongress 2012 (2012), https://doi.org/10.1061/9780784412121.400.
[66] Z. Li, L. Liu, S. Yan, M. Zhang, J. Xia, Y. Xie, Effect of freeze-thaw cycles on mechanical and porosity properties of recycled construction waste mixtures, Constr. Build. Mater. 210 (2019) 347–363.
[67] S. Hao, T. Pabst, Experimental Study and Mathematical Description of Gradation Effect on the Mechanical Characteristics of Crushed Waste Rocks, Int. J. Geomech. 23 (2) (2023) 04022276.
[68] Wen, H., Edil, T.B., 2009. Sustainable Reconstruction of Highways with In-Situ Reclamation of Materials Stabilized for Heavier Loads. BCR2A Conference, Champaign, Illinois, USA.
[69] M. Saberian, J. Li, Long-term permanent deformation behaviour of recycled concrete aggregate with addition of crumb rubber in base and sub-base applications, Soil Dyn. Earthq. Eng. 121 (2019) 436–441.
[70] Domitrović, J., Rukavina, T., Stanislav, L., 2019. Effect of freeze-thaw cycles on the resilient moduli and permanent deformation of RAP/natural aggregate unbound base mixtures. Transportation Geotechnics, 18, 89-91.
[71] P. Ooi, A. Archilla, K. Sandefur, Resilient Modulus Models for Compacted Cohesive Soils, Transp. Res. Record: J. Transp. Res. Board 1874 (2004) 115–124, https://doi.org/10.3141/1874-13.
[72] D. Stolle, P. Guo, Y. Liu, Resilient modulus properties of granular highway materials, Can. J. Civ. Eng. 36 (4) (2009) 639–654.
[73] K. Nokkaew, Characterization of Recycled Aggregate For Use As Base Course Material, GEOMATE 48 (15) (2018). https://doi.org/10.21660/2018.48.pre39.
[74] H.S. Coban, B. Cetin, H. Ceylan, T.B. Edil, W.J. Likos, Evaluation of long-term performance of recycled aggregate base (RAB) layers and optimization of their design thicknesses, Road Mater. Pavement Design (2022) 1–20.
[75] S. Jayakody, C. Gallage, J. Ramanujam, Performance characteristics of recycled concrete aggregate as an unbound pavement material, Heliyon 5 (9) (2019) e02494.
[76] Z. Burtan, D. Chlebowski, The effect of mining remnants on elastic strain energy arising in the tremor-inducing layer, Energies 16 (15) (2022) 6031, https://doi.org/10.3390/en15166031.
[77] T. Rind, A. Jhatial, A. Sandhu, I. Bhatti, S. Ahmed, Fatigue and Rutting Analysis Of Asphaltic Pavement Using "Kenlayer" Software, J. Appl. Eng. Sci. 2 (9) (2019) 177–182, https://doi.org/10.2478/jaes-2019-0024.
[78] D. Balzarini, K. Chatti, I. Zaabar, A. Butt, J. Harvey, Mechanistic-based Parametric Model For Predicting Rolling Resistance Of Concrete Pavements, Transp. Res. Rec. 7 (2673) (2019) 341–350, https://doi.org/10.1177/0361198119847611.
[79] X. Wang, X. Ma, Responses Of Semi-rigid Base Asphalt Pavement With Interlayer Contact Bonding Model, Adv. Civil Eng. 2020 (2020) 1–13, https://doi.org/10.1155/2020/8841139.
[80] D.A. Manuka, T.S. Lachore, Appraising Pavement Surface Distresses and Expected Mitigation Measure On Selected Road Segment, JUSST 08 (23) (2021) 812–823. https://doi.org/10.51201/jusst/21/08466.
[81] L. Bai, Y. Zhang, Analysis Of the Effect Of The Friction Coefficient On A Pavement Structure, Adv. Mater. Sci. Eng. 2022 (2022) 1–17, https://doi.org/10.1155/2022/9285623.
[82] M. Huang, C. Lin, Freeze-thaw Behavior Of Geocell-reinforced Bases Considering Different Fines Contents, Geosynth. Int. 1–18 (2023), https://doi.org/10.1680/jgein.22.00298.
[83] S.E. Haile, Y. Liu, The Effect Of Freeze-thaw On the Performance Of Recycled Concrete Pavement, IJAERS 2 (10) (2023) 001–014. https://doi.org/10.22161/ijaers.102.1.
[84] G. Shu'an, X. Lu, G. Liu, Z. Baoli, Y. Fan, Z. Zheng, Influence Of Freeze-thaw Cycles On Mechanical Response Of Levee Pavement, Adv. Civil Eng. 2021 (2021) 1–10, https://doi.org/10.1155/2021/6639303.
[85] T. Bai, M. Guo, Y. Wei, W. Ma, Impact Of Freeze–thaw Cycles On the Long-term Performance Of Concrete Pavement And Related Improvement Measures: A Review, Materials 13 (15) (2022) 4568, https://doi.org/10.3390/ma15134568.
[86] Y. Yang, Z. Sun, Y. Yang, L. Yue, G. Chen, Effects Of Freeze–thaw Cycles On Performance and Microstructure Of Cold Recycled Mixtures With Asphalt Emulsion, Coatings 6 (12) (2022) 802, https://doi.org/10.3390/coatings12060802.
[87] A. Abdel-hay, Properties of recycled concrete aggregate under different curing conditions, HBRC J. 3 (13) (2017) 271–276, https://doi.org/10.1016/j.hbrcj.2015.07.001.
[88] T. Pavlů, J. Pazderka, K. Fořtová, J. Řepka, D. Mariaková, T. Vlach, The Structural Use Of Recycled Aggregate Concrete For Renovation Of Massive External Walls Of Czech Fortification, Buildings 5 (12) (2022) 671, https://doi.org/10.3390/buildings12050671.
[89] M. Rout, S. Sahdeo, S. Biswas, K. Roy, A. Sinha, Feasibility Study Of Reclaimed Asphalt Pavements (Rap) As Recycled Aggregates Used In Rigid Pavement Construction, Materials 4 (16) (2023) 1504, https://doi.org/10.3390/ma16041504.